Thermal modeling and measurement of a transformer using pcb sensor sheet

Hassan Rouhi

School of Electrical Engineering

Thesis submitted for examination for the degree of Master of Science in Technology.
Espoo 25.07.2019

Supervisor

Prof. Antero Arkkio

Advisor

Ahmed Hemeida, D.Sc.

Aalto University
School of Electrical
Engineering

Aalto University
School of Electrical
Engineering

Aalto University, P.O. BOX 11000, 00076 AALTO
www.aalto.fi
Abstract of the master's thesis

Author Hassan Rouhi

Title Thermal modeling and measurement of a transformer using pcb sensor sheet

Degree programme Automation and electrical enegineering

Major Electrical Power and Energy Engineering **Code of major** ELEC3024

Supervisor Prof. Antero Arkkio

Advisor Ahmed Hemeida, D.Sc.

Date 25.07.2019 **Number of pages** 55 **Language** English

Abstract

A transformer is a device that usually has at least two windings and converts voltage from a level to another level without changing the frequency. Transformers are used widely in the power networks and due to their high price, it is extremely crucial to evaluate their losses, the value of the temperature rise (for protecting the insulation) and their efficiency. The temperature above the limit may leads to serious damage in the transformer components. Traditional way of obtaining the total power loss in a transformer is subtracting the output power from the input power with the help of a power analyzer. But high harmonics can affect the quality of the measurements and as a result, leads to inaccurate power loss calculation. This thesis aims to develop a thermal model in COMSOL and find the value of temperature rise in the transformer and compare it with the temperature rise in the lab. The losses of the transformer can be calculated inversely from the value of the temperature rise. The measurements in different conditions and at different frequencies are done in the lab and the core loss obtained by the method discussed in chapter 3. Secondly, the electromagnetic model of the transformer in COMSOL is developed to obtain the core loss of the transformer and compare it with the core loss obtained from the measurements. Finally, the thermal model of the transformer is developed in COMSOL and the values of the core loss obtained from the electromagnetic model injected into the thermal model for estimating the temperature rise in the transformer. The temperature rise verified by the temperature rise measurement in the lab. Two PT-100 temperature sensors are used for the measurements in the lab. The sensors are located in the middle of the transformer and the temperature was read by Agilent 34970 A. The results obtained from both the electromagnetic model and thermal model are in good agreement with the results from the measurement.

Keywords Finite element method, thermal model, electromagnetic model, power measurements

Preface

I would like to express my sincere and respectful thanks to my supervisor Prof. Antero Arkkio for giving me this opportunity to work in his research group. My thanks also go to my advisor Ahmed Hemeida for his supportive approach as an advisor and for his comprehensive support in my whole thesis. I appreciate Ari Haavisto for his great help during the thesis in the lab. I am grateful to all my friends and colleagues in the Electrical engineering school of Aalto University. Last but not least, I would like to thanks my parents and my beloved wife for their great supports.

Otaniemi, 25.07.2019

Hassan Rouhi

Contents

Symbols and Abbreviations

Symbols

α	Temperature coefficient of resistance for copper
ΔT	Temperature change
ε	Permittivity
ϵ	Emissivity of the radiating surface
η	Efficiency
η_{fe}	Filling factor of the core
η_{cu}	Filling factor of the winding
θ	Temperature
λ	Thermal conductivity
μ_0	Permeability of the free space
μ_{r}	Permeability of the material
ρ_{cu}	Resistivity of the copper
ρ	Electric Charge
ρ_{wp}	Mass density of the primary winding
ρ_{ws}	Mass density of the secondary winding
ρ_{c}	Mass density of the copper
ρ_{a}	Mass density of the air
σ_{B}	Stefan-Boltzmann constant
σ	Conductivity
φ	Magnetic flux
ω	angular frequency
a	Turn ratio of the transformer
A_{core}	cross-sectional area of the core
A_{w1}	Cross area of the wires in the primary side
A_{w1eff}	Effective cross area of the wires in the primary side
A_{c1}	Cross area of one wire in the primary side
A_{cv}	Surface area of the surface exposed to the fluid flow
B_{max}	Maximum value of the flux density in the core
$\mathbf{B}$	Magnetic flux density
C	Capacitance
C_{th}	Thermal capacitance
C_{pwp}	Heat capacity of the primary winding
C_{pws}	Heat capacity of the secondary winding
C_{pc}	heat capacity of the copper
C_{pa}	heat capacity of the air
C_{p}	Heat capacity
d_{w1}	Diameter of the wire in the primary side
$\mathbf{D}$	Electric flux density
$e_1(t)$	Induced voltage in primary winding
$e_2(t)$	Induced voltage in secondary winding
$\mathbf{E}$	Electric field
f	Frequency
f_{p}	Filling factor for primary
f_{s}	Filling factor for secondary
G	Conductance

G_{th}	Thermal conductance
h_{c}	Heat transfer convection coefficient
$\mathbf{H}$	Magnetic field intensity
$i_1(t)$	Current in the primary winding
$i_2(t)$	Current in the secondary winding
I_{tot}	Total value of current following in the windings
J_{cu}	Current density
J^T	Transpose of Jacobian matrix
$k_{\mathrm{h_c}}$	Thermal conductivity of the copper
$k_{\mathrm{h_a}}$	Thermal conductivity of the air
k_{hwp}	Primary winding thermal conductivity
k_{hws}	Secondary winding thermal conductivity
k_{ij}	Second order thermal conductivity tensor
k_{h}	Thermal conductivity of the material
K_{h}	Hysteresis coefficient
K_{e}	Eddy current loss coefficient
l_1	Length of one turn of wire in the primary side
l_{tot}	Total length of wire required in the primary side
l_{c}	Mean path length of the core
n	Steinmetx exponent
N_{p}	Number of primary winding turns
N_{s}	Number of secondary winding turns
$N_1(t)$	Number of primary winding turns
$N_2(t)$	Number of secondary winding turns
N_{aux}	Number of turns of the auxiliary coil
P_{res1}	Resistive loss of the primary winding
P_{res2}	Resistive loss of the secondary winding
P_{core}	Core loss
P_{h}	Hysteresis loss
P_{e}	Eddy current loss
P_{in}	Input power
P_{out}	Output power
q	Heat flux
q_{h}	Conduction heat transfer rate
Q_{h}	Power generated per unit volume
Q	Heat
R_{th}	Thermal resistance
R_1	Primary resistance
R_2	Secondary resistance
R_{c}	Core loss resistance
t	Time instant
T_{s}	surface temperature
T_{amb}	ambient temperature
V_{rms}	root mean square value of the voltage over the primary winding
V_{p}	Primary voltage
V_{s}	Secondary voltage
$V_1(t)$	Voltage in the primary winding

$V_2(t)$	Voltage in the secondary winding
V_{d1}	Voltage drop in the primary winding
V_{aux}	Voltage of the auxiliary coil
X_1	Primary leakage reactance
X_2	Secondary leakage reactance
X_{m}	Magnetizing reactance

Abbreviations

AC	Alternating current
PCB	printed circuit board
PWM	Pulse-width modulation
RMS	Root mean square

1 Introduction

1.1 Transformer – An Overview

Micheal Faraday in 1831 had revealed the principles of transformers, and later an American physicist William Stanley Jr. made the first commercial version of a transformer in 1886. A transformer is a device that can change electric power from a specific frequency and voltage level to another voltage level at the same frequency. In general, transformers work based on mutual induction. A basic transformer has at least two windings. The simplest case of a transformer has been shown in figure 1.1 with N_{p} as a number of primary winding turns and N_{s} as a number of secondary winding turns where V_{p} and V_{s} are the primary and secondary voltage respectively. The number of turns in primary and secondary can be achieved by equation (1-1) [1].

$$N_{\mathrm{p}} = \frac{\sqrt{2}\,V_{\mathrm{rms}}}{2\pi f B_{\mathrm{max}} A_{\mathrm{core}}} \tag{1-1}$$

where V_{rms} is the root mean square value of the voltage over the primary winding, B_{max} is the maximum value (peak value) of the flux density in the core, A_{core} is the cross-sectional area of the core and f is the frequency.

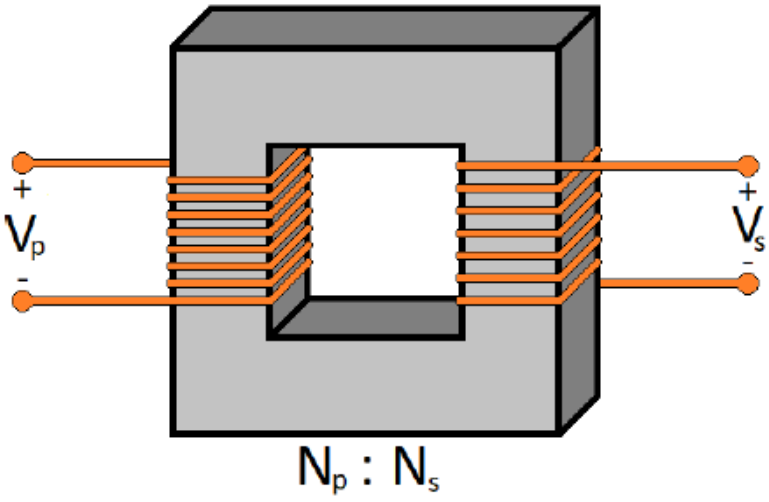

Figure 1.1: A single-phase transformer

From the different parts of a transformer, magnetic cores are one of the most important parts of a transformer. Their main duty is to transfer flux from the primary winding to the secondary winding of the transformer. When magnetic materials are subjected to a time-varying magnetic

flux, core loss occurs [2]. The usual method for obtaining the losses in a transformer is the difference between input and output power measured by a power analyzer or any other measuring device. However, there is a big drawback in this method. To accurately measure the core losses, the winding losses have to be subtracted from the power losses measured from the power analyzer. Although, these power losses are temperature dependent. In addition, if the transformer is fed from a PWM inverter fed supply, the power analyzer becomes inaccurate in power losses computation and high harmonics affect the quality of the measurement. Therefore, inverse thermal modeling can be used to study the coupling between the electromagnetic and thermal model of a transformer. Afterward, the core losses can be computed inversely using the inverse method. Temperature is measured by a PCB sheet that contains the PT 100 sensors. The above issues cannot have an effect on the temperature rise in the transformer core and the calculation of the core losses is more accurate [3].

1.2 Aim of the Thesis

The motivation behind the thesis is to create a thermal model of a single-phase transformer with COMSOL Multiphysics® and find the core loss in the transformer core inversely from the temperature rise of the transformer core.

The primary objectives of the thesis are as follows:

- To study and develop electromagnetic model of the transformer and obtain core loss with the model. Then compare it with the core loss calculation based on the measurement in the lab.
- To study and develop thermal model of the transformer and inject the core loss obtained from electromagnetic model to the thermal model in order to find the temperature rise in the transformer.
- To compare the temperature rise by measurement in the lab with the temperature rise obtained from the thermal model.

1.3 Thesis Structure

This thesis contains six chapters. Chapter 1 gives an overview and the main objectives of the thesis. In chapter 2, some background literature studies of the transformer and different losses in the transformer are discussed. In chapter 3, a method for designing the transformer has been introduced and the method for obtaining the value of hysteresis and eddy current loss coefficient are discussed in this chapter. Chapter 4 contains the electromagnetic model of the transformer and a comparison between the core loss values from the model and measurement in the lab. The thermal model of the transformer in COMSOL Multiphysics® is discussed in chapter 5 of the thesis. Chapter 6 contains the conclusion and future work.

2 Theoretical Background

2.1 Transformer

Transformers are playing a vital rule in modern life. They are available in different sizes, from small scale to very large size and capacity. But the principles of all transformers are almost the same. As a basic definition, transformers change the level of voltages using magnetic induction. The frequency remains unaffected with changing the voltage level. The simplest transformer has two or more windings wounded around the core. The primary winding connects to the voltage supply and one or more windings connect the secondary to the load. Faraday's induction law is the basic principle of the transformers. The coils are not connected electrically but are magnetically linked through the core. For decreasing the core loss, the core consists of steel lamination instead of a solid core. The laminations are isolated electrically in order to reduce the eddy current loss in the core. When a current passes through the primary winding, a magnetic field inside the core is created. This magnetic field induces a voltage in the secondary winding as shown in figure 2.1.

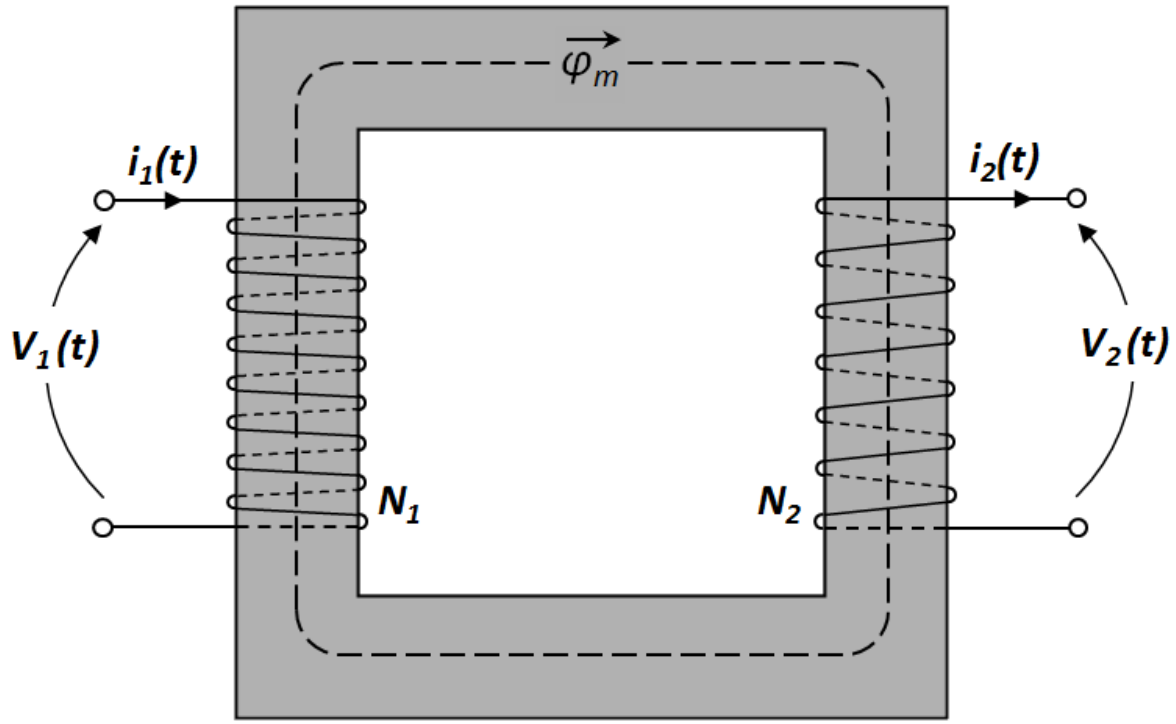

Figure 2.1: Single-phase transformer

2.2 Ideal Transformer

Figure 2.2 shows the schematic of an ideal transformer where there is no loss in the transformer.

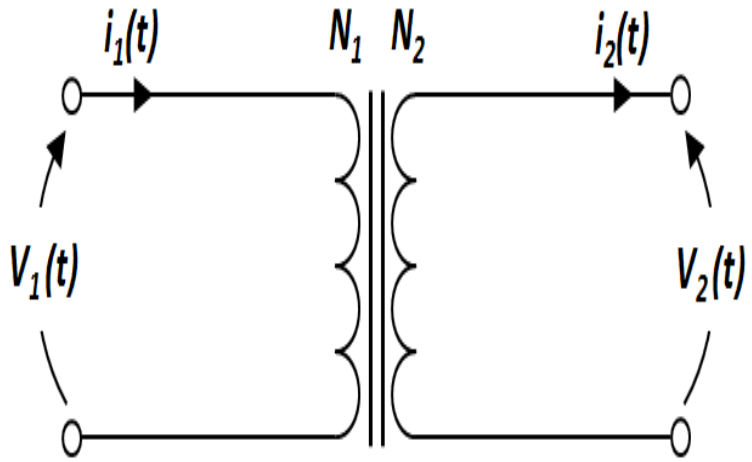

Figure 2.2: Ideal transformer

In figure 2.2:

- t is the time instant
- $V_1(t)$ is the voltage in the primary side
- $V_2(t)$ is the voltage in the secondary side
- $i_1(t)$ is the primary current
- $i_2(t)$ is the secondary current
- N_1 is the number of turns on the primary side
- N_2 is the number of turns on the secondary side

The value of induced voltage is proportional to the number of turns linked by the magnetic flux, based on the Faraday's induction law [4]. Therefore the value of the primary and secondary voltages are proportional to the number of turns in primary and secondary.

$$a = \frac{V_1}{V_2} = \frac{N_1}{N_2} \tag{2-1}$$

a is the transformer turn ratio. The relationship between the currents of the transformer and the number of turns can be like equation (2-2).

$$\frac{i_2}{i_1} = \frac{N_1}{N_2} = a \tag{2-2}$$

By considering the Faraday's induction law again, the equations for obtaining the induced voltages in the transformer primary and secondary sindings are like equations 2-3 and 2-4, respectively.

$$e_1 = N_1 \frac{d\varphi}{dt} \tag{2-3}$$

$$e_2 = N_2 \frac{d\varphi}{dt} \tag{2-4}$$

where φ is the magnetic flux in the core.

As there is not any loss in the ideal transformer, the values of induced voltages e_1 and e_2 are the same as primary and secondary voltage, V_1 and V_2 respectively. As a result, the relationship between the induced voltages, primary and secondary voltages, primary and secondary currents and the number of turns are

$$\frac{V_1}{V_2} = \frac{e_1}{e_2} = \frac{i_2}{i_1} = \frac{N_1}{N_2} = a \tag{2-5}$$

The equation for magnetic flux is as follow

$$\varphi(t) = \varphi_{\mathrm{p}} sin\omega t \tag{2-6}$$

where φ_{p} is the peak value of the flux and ω is the angular frequency.

Equation (2-6) is valid when the excitation voltage in the primary is sinusoidal. By using equation (2-6) in equation (2-4)

$$e_2 = N_2 \frac{d\varphi}{dt} = N_2 \omega \varphi_{\mathrm{p}} cos\omega t \tag{2-7}$$

The equation (2-7) could be used for finding the RMS value of the induced voltage in the secondary when the secondary winding is left open and the load is not connected to the secondary side.

$$e_{2\mathrm{rms}} = \frac{N_2 \omega \varphi_{\mathrm{p}}}{\sqrt{2}} = \frac{2\pi f N_2 \varphi_{\mathrm{p}}}{\sqrt{2}} \tag{2-8}$$

The peak value of flux density in the core is given by

$$B_{\mathrm{p}} = \frac{\varphi_{\mathrm{p}}}{A_{\mathrm{core}}} \tag{2-9}$$

Where A is the cross-sectional area of the core. Therefore, we can find the equation for peak flux density in the core as equation (2-10) [4].

$$B_{\mathrm{p}} = \frac{\sqrt{2}\, e_{2\mathrm{rms}}}{2\pi f N_2 A_{\mathrm{core}}} \tag{2-10}$$

2.3 Equivalent Circuit of Transformer

There is not an ideal transformer in practice. In an ideal transformer, we have the following assumption:

- The transformer does not need magnetizing current in order to set up the magnetic flux.
- Hysteresis and eddy current loss in the magnetic core is zero.
- Magnetic permeability is infinite. So leakage inductance can be zero.
- There is no loss in the winding. So copper loss supposed to be zero in the ideal transformer.

But in a real transformer, we have finite value for permeability in the core, leakage fluxes in primary and secondary windings, winding resistances and core loss that lead to losses in the transformer. As we discussed earlier, the magnetic permeability of the core is finite. Therefore, some fluxes scape from the core and will not pass through both windings. They are known as the leakage flux. This produces a self-inductance in the primary and secondary windings. The primary and secondary flux leakage, $\varphi_{11}$and φ_{22} are shown in Fin. 2.3.

In the real transformer equivalent circuit, we consider magnetizing current as well. The magnetizing or excitation current can be modeled as a parallel reactance to the primary windings. Then, the copper loss is considered in the transformer by a series resistance for each winding [5].

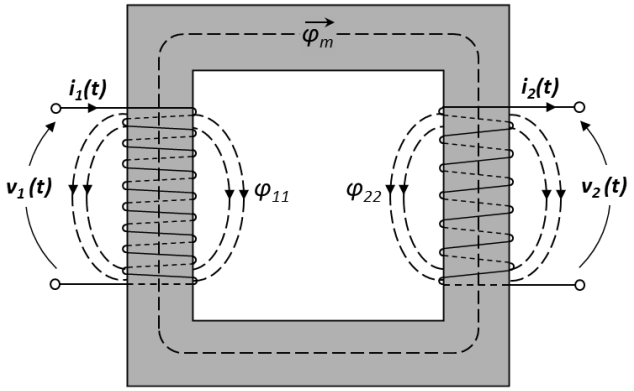

Figure 2.3: Transformer with flux leakage in the primary and secondary winding [4]

Figure 2.4 presents the equivalent circuit for the practical transformer. The circuit considered the core loss, exciting reactance, self-inductance and the resistances in the primary and secondary.

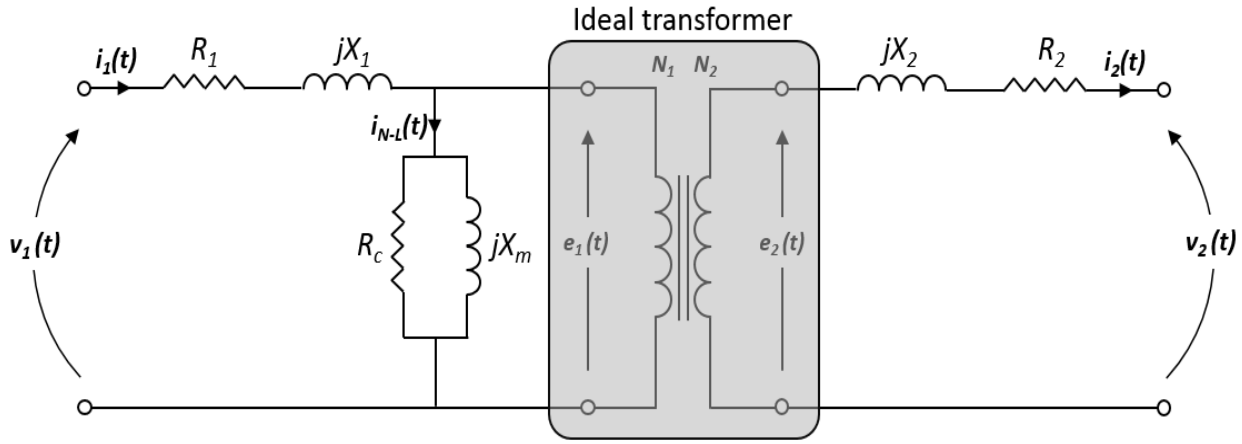

Figure 2.4: Equivalent circuit of a practical transformer [4]

Where

- $V_1(t)$ is the primary voltage
- $V_2(t)$ is the secondary voltage
- R_1 is the primary resistance
- R_2 is the secondary resistance
- X_1 is the primary leakage reactance
- X_2 is the secondary leakage reactance
- R_{c} is the core loss resistance
- X_{m} is the magnetizing reactance

2.4 Losses in the Transformer

A transformer is static electrical equipment. Therefore, it does not have mechanical losses like electrical machines. However, in the practical transformer, there is electrical loss which can be divided into two main groups. The first group is magnetic power loss that is known as core loss or iron loss and the second is copper loss or ohmic loss.

2.4.1 Hysteresis Loss

Magnetic core in a transformer usually is made of silicon steel. Ferromagnetic materials have domains in their instruction that are located in a random direction when the material is non-magnetized. The resultant magnetic field in a non-magnetized ferromagnetic material is zero.

A ferromagnetic material that has never been magnetized before follows curve ab when an external field is applied to it. If the value of the H is increased, flux density increases and will reach to the point "a". If the external field is removed, magnetic intensity H becomes zero, but the core has still some fluxes which are known as the residual flux density. The residual flux density causes the material to become magnetized permanently. In order to return all domains to their random position, a magnetic field in a reverse direction is needed. This opposite magnetic field is demagnetizing process. Based on figure 2.5, point " a " shows the instant when all domains in the material are arranged randomly. Point " b " is when the material reaches saturation, and finally, the path " c-d " illustrates the demagnetizing process. If alternating magnetic field applies to the material, in every cycle demagnetizing process must be repeated which requires the consumption of electrical power that is hysteresis loss [7]. The Empirical equation (2-11) calculates the value of the total hysteresis loss [8]:

$$P_{\mathrm{h}} = K_{\mathrm{h}} B_{\mathrm{max}}^{n} f \tag{2-11}$$

Where

- K_{h} is hysteresis coefficient depending on the characteristics of the material
- B_{max} is the maximum of flux density
- f is the frequency of supply current
- P_{h} is hysteresis loss
- n is Steinmetz exponent

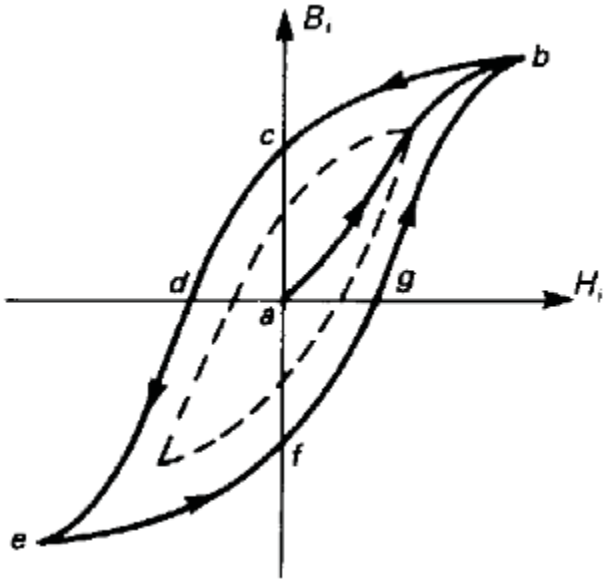

Figure 2.5: B-H loop of ferromagnetic material [6]

2.4.2 Eddy Current Loss

When an alternating magnetic field excites windings, it induces an *emf* in the coils based on the Faraday's induction law and as a result *emf* is induced in the core also. Magnetic materials are good conductor also, so the induced *emf* can create a current inside the core along a closed path [7]. This induced current is known as eddy current. The resistance of the closed current path is high and therefore, the induced eddy current can show its effect. Heating of the core is the most important effect of the eddy current which represents the loss in the core which is known as eddy current loss [9].

With the help of equation (2-12), we can have a good estimation for eddy current loss:

$$P_{\mathrm{e}} = K_{\mathrm{e}} B_{\mathrm{max}}^2 f^2 \tag{2-12}$$

where

- K_{e} is the eddy current loss coefficient depending on the material
- B_{max} is the maximum of flux density
- f is the frequency of supply current
- P_{e} is the eddy current loss.

2.4.3 Stray Loss

The main loss components of a transformer are core loss and copper loss. But besides these two losses, there is a loss component which is called stray loss. Leakage flux in a transformer can induce a voltage, and therefore a current will be produced in the conductor, tanks, etc. This eddy current will produce a loss in the transformer [5].

2.4.4 Dielectric Loss

Dielectric loss occurs in the transformer insulation. Dielectric loss is important in the case of a high voltage transformer.

Stray loss and dielectric loss are usually small and they are negligible in efficiency calculation [5].

2.5 Transformer Efficiency

Due to the presence of core loss in the transformer and copper loss is the primary and secondary windings, a portion of the power dissipated in the transformer that shows itself as heat. Generally, efficiency is defined as the ratio of the output power to the input power [8].

$$\eta = \frac{P_{\text{out}}}{P_{\text{in}}} = \frac{P_{\text{out}}}{P_{\text{out}}+P_{\text{loss}}} \tag{2-13}$$

Efficiency can be expressed as percentage:

$$\eta\% = \frac{P_{\text{out}}}{P_{\text{in}}} \times 100 \tag{2-14}$$

3 Methods for Transformer Design and Calculating Losses in the Transformer

3.1 Designing the Transformer

Different steps for designing a transformer are discussed in this chapter. For designing a transformer, there are four main parameters that should be found:

- Number of turns in the primary side
- Number of turns in the secondary side
- Diameter of the conductor for the primary winding
- Diameter of the conductor for the secondary winding

There are some constraints for designing the transformer that is discussed in this chapter.

3.1.1 Number of Turns in the Primary Winding

The transformer designed with the following input constraints:

- The frequency is f =50 Hz
- The rated primary voltage V_1 =24 V
- Flux density at no-load is B =1.4 T
- The filling factor of the core is η_{fe}=0.94
- The value of the current density is J_{cu}=0.65 $\frac{A}{mm^2}$

The number of turns in the primary is calculated as:

$$N_1 = \frac{\sqrt{2}\,V_1}{\omega B A_{\text{fe}}} \tag{3-1}$$

where the flux density in order to design the transformer is 1.4 T and A_{fe} is equal to 406×10^{-6} m^2.

Therefore, the value of primary turns equals to 190.

At least 3% voltage drop is added to the number of primary windings. Therefore, the number of turns in the primary is adjusted to 195.

3.1.2 Diameter of the Wire

In order to obtain the diameter of the copper wire, the cross area of the wires based on the schematic of EI core in figure (3.1) equals:

$$A_{\text{w1}} = Z_1 \left(\frac{\text{CC}-\text{AA}}{2} - \text{S}\right) \tag{3-2}$$

Table 3.1: Dimensions of EI-plate

	A mm	B mm	C mm	AA mm	BB mm	CC mm	D mm	L mm	LL mm	S mm	Z1 mm	Z2 mm
EI 60	60.0	40.0	10.0	20.6	21.0	39.0	42.5	27.0	29.0	1.1	12.9	12.9

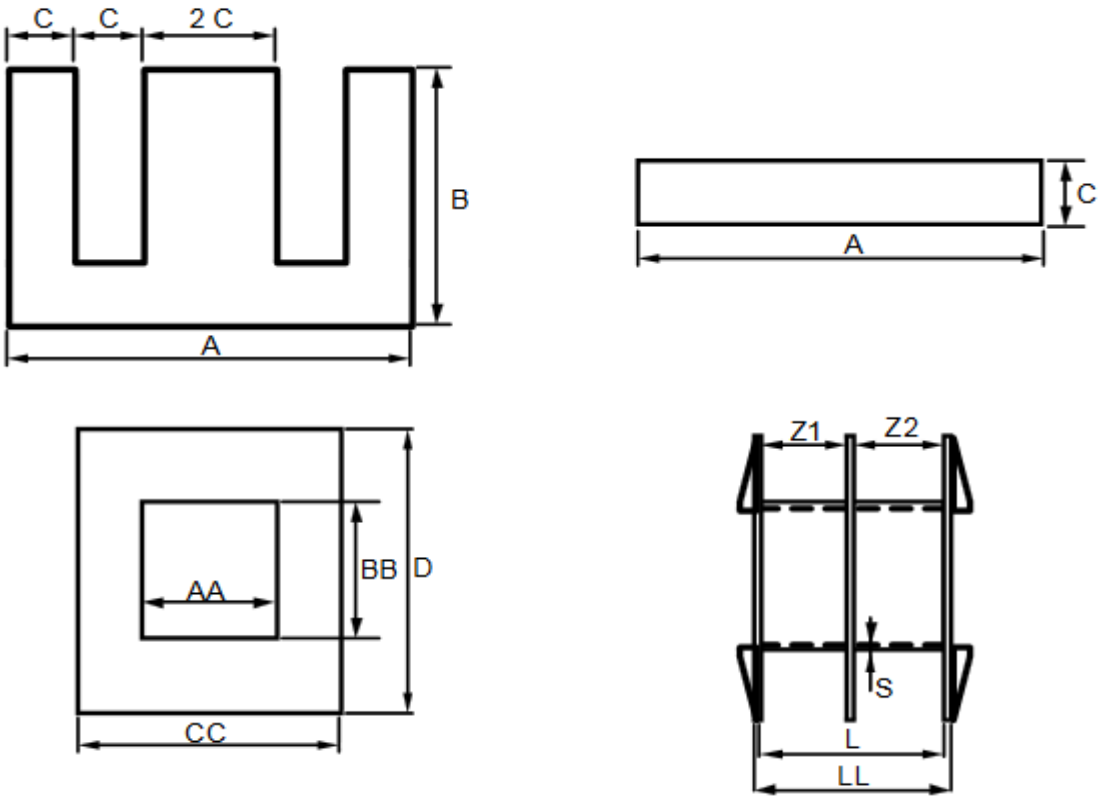

Figure 3.1: Schematic of the EI core

Table 1.1 shows the dimensions of the transformer sheets (EI 60). By substituting the values from table 3.1:

$$A_{w1} = 104.49 \times 10^{-6}\ \mathrm{m}^2 \tag{3-2}$$

We supposed that the filling factor of the windings is 0.65 ($\eta_{cu} = 0.65$). Therefore, the effective cross area of the wires is

$$A_{w1eff} = \eta_{cu} A_{w1} = 67.91 \times 10^{-6}\ \mathrm{m}^2 \tag{3-3}$$

Therefore, the area of one wire is

$$A_{c1} = \frac{A_{w1eff}}{N_1} = 0.34 \times 10^{-6}\, m^2 \quad (3\text{-}4)$$

Equation (3-5) gives the value of the wire diameter that we need to use for windings

$$d_{w1} = 2\sqrt{\frac{A_{c1}}{\pi}} \quad (3\text{-}5)$$

Therefore, the diameter of one wire is 0.63 mm. However, a high filling factor is required in order to have 195 turns on the primary side of the transformer which is almost impossible due to the size of the bobbin. One solution is to use a wire with a smaller diameter. On the other hand, the value of flux density will reduce when a wire with a smaller diameter is used. As a result, the number of turns in the primary side of the transformer was increased to 207 turns in order to have flux density equal to 1.4 T in the core.

3.1.3 Number of Turns in the Secondary Windings

Based on the table 3.1, the length of one turn of wire calculated by (3-6).

$$l_1 = 2(AA + BB + 4s) \quad (3\text{-}6)$$

Therefore, the length of one turn of wire required in windings is 92 mm. The total length of wire required in the primary winding is

$$l_{tot} = N_1 l_1 = 19.04 \text{ m} \quad (3\text{-}7)$$

Resistivity of the copper wire (ρ_{cu}) at 20 °C is 0.0711 Ω/m. It is supposed that the average temperature rise in the windings at different frequencies is 100 °C. Therefore, the resistivity of the copper wire at 100 °C is:

$$\rho_{cu100} = \rho_{cu20}(1 + \alpha\, \Delta T) = 0.0934\ \frac{\Omega}{m} \quad (3\text{-}8)$$

where α is the temperature coefficient of resistance for copper

ΔT is the temperature change

ρ_{cu20} is the resistivity of the copper wire at 20 °C

Primary winding total resistance is calculated by (3-9).

$$R = l_{tot}\rho_{cu100} = 1.77\ \Omega \quad (3\text{-}9)$$

The effective value of the current density (J_{cu}) and the copper cross-section area (A_{cu}) based on the table in Appendix B is 0.246 mm^2. Therefore, the value of the rated current in the primary winding is:

$$I = J_{cu}A_{cu} = 1.476 \text{ A} \quad (3\text{-}10)$$

The voltage drop in the primary windings is calculated by the equation (3-11).

$$V_{d1} = RI = 2.61\,V \tag{3-11}$$

Finally, the number of turns in the secondary windings:

$$N_2 = N_1 \frac{V_2 + \frac{V_{d1}}{2}}{V_1} = 115 \tag{3-12}$$

3.2 Equipment Used For Measurement

Following is the list of equipment that we used for the experiments in the lab. Also, a short explanation about how we used these devices in the experiments is presented. Figure 3.2 shows the photo of devices that were used during the measurements in the lab.

3.2.1 Amatek CSW 5550

CSW series represents the AC/DC power sources with the ability of variable frequency from 40 up to 5000Hz. In this thesis, the measurements were done in different voltages and frequencies. Therefore, Amatek CSW 5550 was our power source during the measurements.

3.2.2 Norma Power Analyzer D 6100

In order to measure the required parameter during the experiments, we used Norma power analyzer D 6100 which has the ability to have three channels at the same time on its screen. The power analyzer is used for measuring the value of the primary and secondary currents, primary and secondary voltages, primary and secondary powers.

3.2.3 Temperature sensor

PT 100 temperature sensors are used in order to measure the temperature rise in the transformer. Each temperature sensor sheet has ten temperature sensors that give us the temperature rise in different parts of the transformer core.

3.2.4 PCB board

PCB board is used for reading the data from the temperature sensors inside the transformer. Each temperature sensor sheets connected to a separate PCB board.

3.2.5 Insulator

Temperature sensors inside the transformer may have contact with core sheets. This contact leads to short circuit over the sensors and as a result, incorrect value for temperature. In order to avoid these types of issues, we used plastic insulator over both sides of the temperature sensors sheets and then, locate the sheets inside the transformer.

3.2.6 Agilent 34970 A

Agilent 34970 A is a data acquisition device that was used during temperature rise measurements in the lab. Data from the temperature sensors sheets inside the transformer are read and saved in the computer by Agilent 34970 A.

(a)

(b)

(c)

(d)

Figure 3.2: Devices used for the measurements

(a) Agilent 34970 A (b) Amatek CSW 5550
(c) Norma Power Analyzer (d) PCB board

3.3 B-H Curve of the Core

Equation (3-13) is Ampere's law about magnetic field production by a current-carrying wire.

$$\oint \boldsymbol{H}.d\boldsymbol{l} = I_{\text{total}} \tag{3-13}$$

Where

- $\boldsymbol{H}$ is the magnetic field intensity
- $d\boldsymbol{l}$ is the differential element of length
- I_{total} is the total value of current following in the winding

If we suppose all of the magnetic field produced by the current remains in the core, l_{c} is the mean path length of the core. In addition, we assume that the winding has *N* turns. Therefore, Ampere's law becomes:

$$H.l_{\text{c}} = Ni \tag{3-14}$$

Thus, the equation (3-15) becomes available for calculating the value of magnetic field intensity:

$$H = \frac{Ni}{l_{\text{c}}} \tag{3-15}$$

The materials used in the core can also affect the value of magnetic field intensity.

Equation (3-16) shows the relationship between flux density (B) and magnetic field intensity [8].

$$B = \mu H = \mu_0 \mu_{\text{r}} H \tag{3-16}$$

Where

μ_0 is the absolute permeability of free space and it is equal to $4\pi \times 10^{-7}\text{H/m}$

μ_{r} is relative permeability of the material

The B-H curve of a magnetic material is the plot of the flux density versus magnetic field intensity. Figure (3.3) shows the magnetization curve or B-H curve for 50 Hz.

Throughout this thesis, we used the auxiliary coil for calculating the flux density in the core [10]. The auxiliary coil has ten turns and wound around one limb of the core. Equation (3-17) shows the equation for finding the flux density in the auxiliary coil.

$$b_{\text{fe}} = \frac{\sqrt{2}\, V_{\text{aux}}}{2\pi f N_{\text{aux}} (\frac{A_{\text{fe}}}{2})} \tag{3-17}$$

Where

- V_{aux} is the value of the induced voltage in the auxiliary coil
- N_{aux} is the number of turns in the auxiliary coil which is 10 throughout the thesis

The cross-sectional area of the core is divided by two in equation (3-17) because the cross-sectional area of the side limb is half of the middle limp and the auxiliary coil wounded over the side limb.

Equation (3-15) is used for calculating the magnetic field intensity. Figure (3.3) shows the magnetization curve for 50 Hz at no-load condition. The voltage source is connected to the primary winding and the secondary winding is left open.

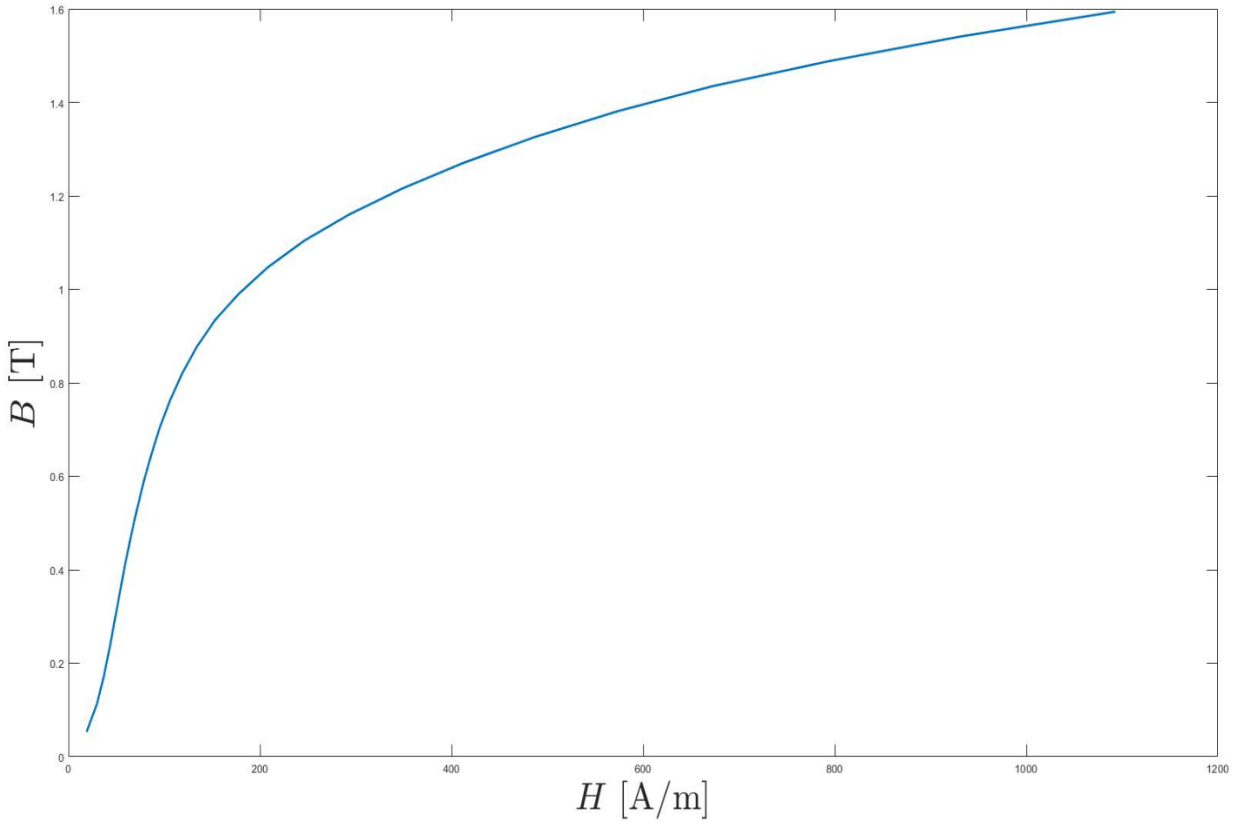

Figure 3.3: Magnetization curve of the core at 50 Hz

3.4 Method for Measuring the Core Loss

As discussed earlier, two types of losses are assumed in the thesis. Core losses and winding losses. Core losses include eddy current loss and hysteresis loss. Winding losses occur in the winding and it is proportional to the resistance of the winding and square of currents. Here, the method used for calculating the core losses based on the measurement result is presented. The calculation is presented in the no-load and loaded conditions.

3.4.1 Transformer in no-load condition

Figure 3.4 illustrates the transformer circuit diagram of the transformer at no-load condition. The secondary winding is left open and 24 volts are supplied to the primary windings. No

current flows through the secondary winding and the resistive loss is considered zero in the secondary winding. The copper or resistive loss in the transformer is calculated by (3-18).

$$P_{\text{res1}} = R_1 i_1^2 \tag{3-18}$$

With ignorance of small losses like stray loss or dielectric loss in the transformer, the core loss in the transformer can be calculated by equation (3-19)

$$P_{\text{core}} = P_1 - P_{\text{res1}} \tag{3-19}$$

Where P_1 is the primary power read by the power analyzer.

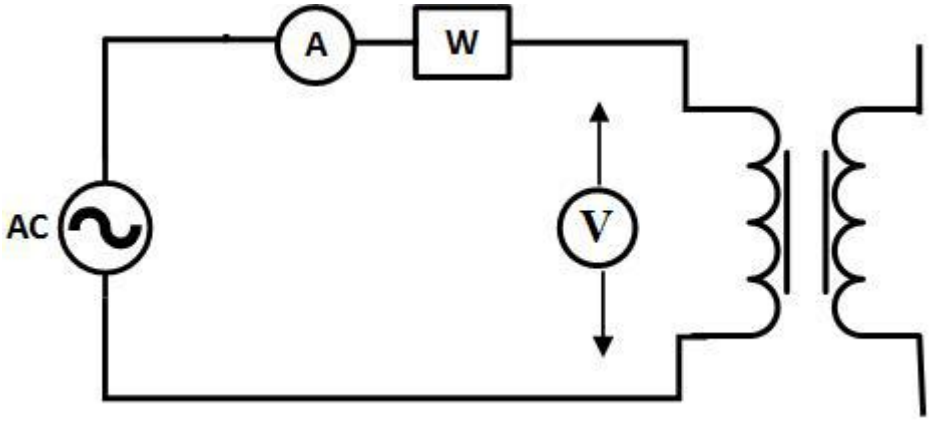

Figure 3.4: Transformer circuit in no-load connection

Figure 3.5 shows the no-load core loss at different frequencies in the transformer.

3.4.2 Transformer in loaded condition

In the second connection, a constant load is connected to the secondary windings. For finding the value of the load resistance, the rated voltage is supplied to the primary windings (24 V at 50 Hz) and load resistance is adjusted in order to have the rated current in the primary windings (1.47 A). The primary voltage is changed and the primary and secondary currents, secondary voltage and primary and secondary powers are measured.

The resistive loss in the primary is calculated the same as no-load condition and the secondary resistive loss is calculated by (3-20).

$$P_{\text{res2}} = R_2 i_2^2 \tag{3-20}$$

Moreover, the core loss in the transformer is calculated by (2-21):

$$P_{\text{core}} = P_1 - P_2 - (P_{\text{res1}} + P_{\text{res2}}) \tag{3-21}$$

Figure 3.6 displays the core loss in different frequencies when the load is connected to the secondary windings.

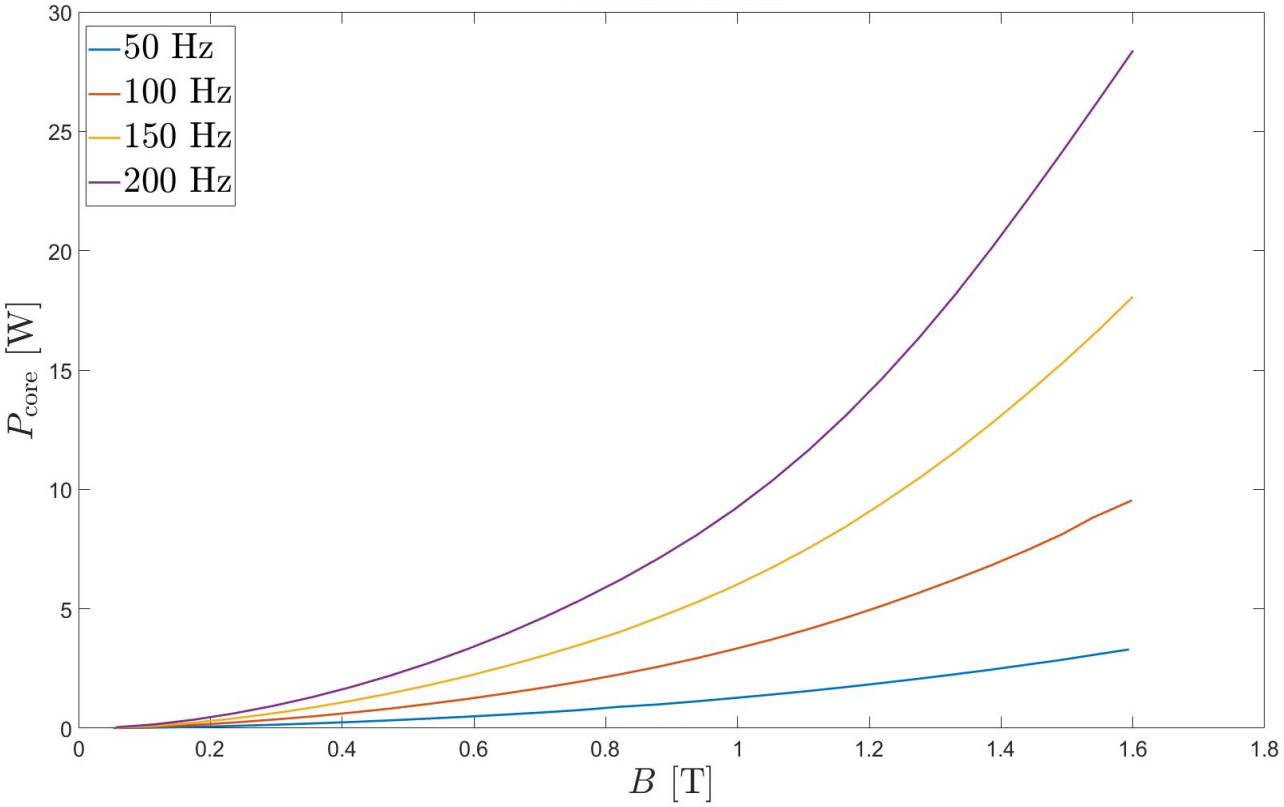

Figure 3.5: Core loss at no load condition

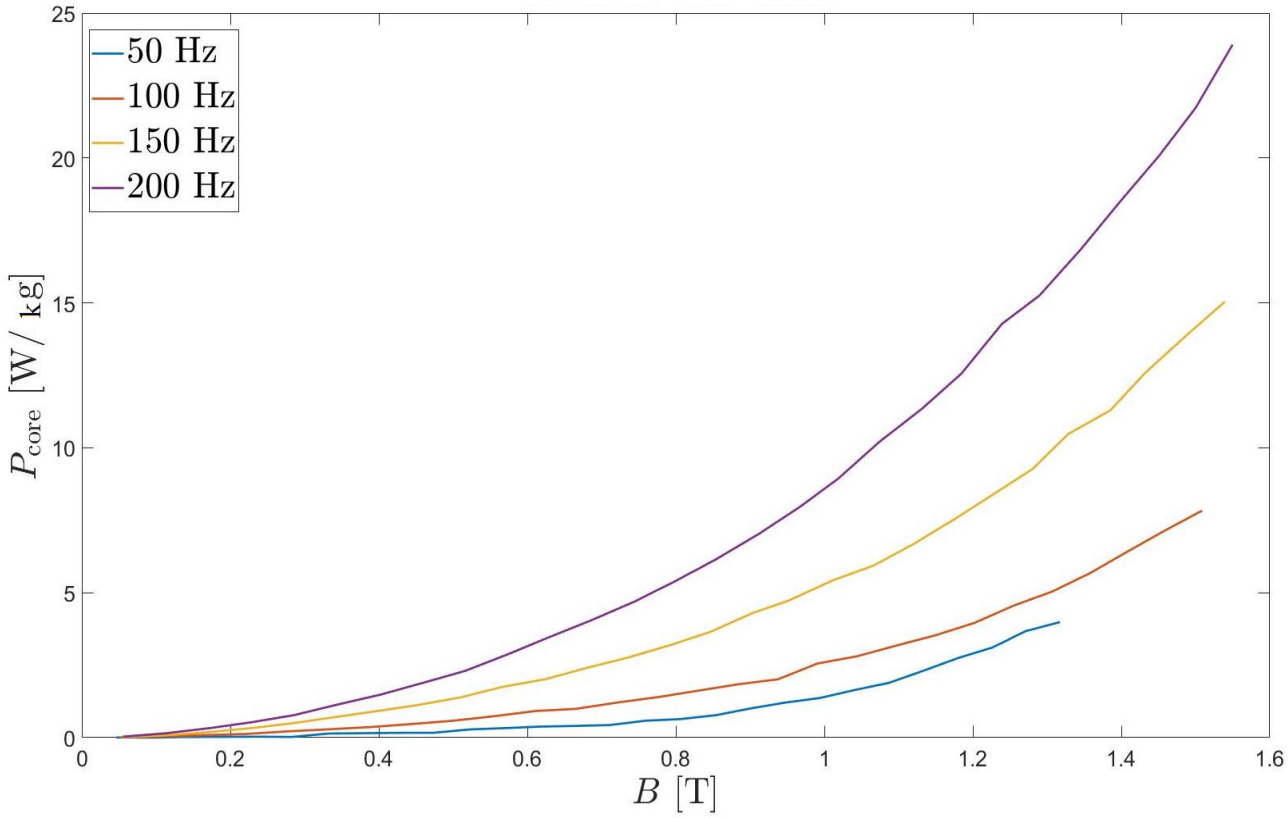

Figure 3.6: Core loss at loaded condition

3.5 Eddy and Hysteresis Coefficient

Core loss in a magnetic core happens when a varying magnetic flux is applied to the magnetic material. As discussed earlier, the core loss is divided into two components. The excess loss is ignored throughout this thesis. According to the Steinmetz equation, the core loss with a sinusoidal flux density of varying magnitude and frequency as supply is calculated based on the equation (3-22).

$$P_{\text{core}} = P_{\text{h}} + P_{\text{e}} = K_{\text{h}} B_{\text{max}}^{n} f + K_{\text{e}} B_{\text{max}}^{2} f^{2} \tag{3-22}$$

where K_{h}, K_{e} and n are the coefficients, which depend on the lamination material, thickness, conductivity and etc [11]. In order to find the hysteresis coefficients, equation (2-11) was used. The majority of the core loss was supposed hysteresis loss at very low frequency. So the measurement was done at no-load condition at 10 Hz as a supply frequency and the core loss was calculated based on the method in the previous section. The value of the calculated core loss is considered equal to the hysteresis loss. Therefore, the equation (3-23) is used for fitting the curve in MATLAB in order to find the hysteresis coefficients.

$$P_{\text{h}} = K_{\text{h}} B^{n} f \tag{3-23}$$

where we need to find the values of K_{h} and n. Figure 3.7 shows the fitted curve where core loss plotted versus flux density.

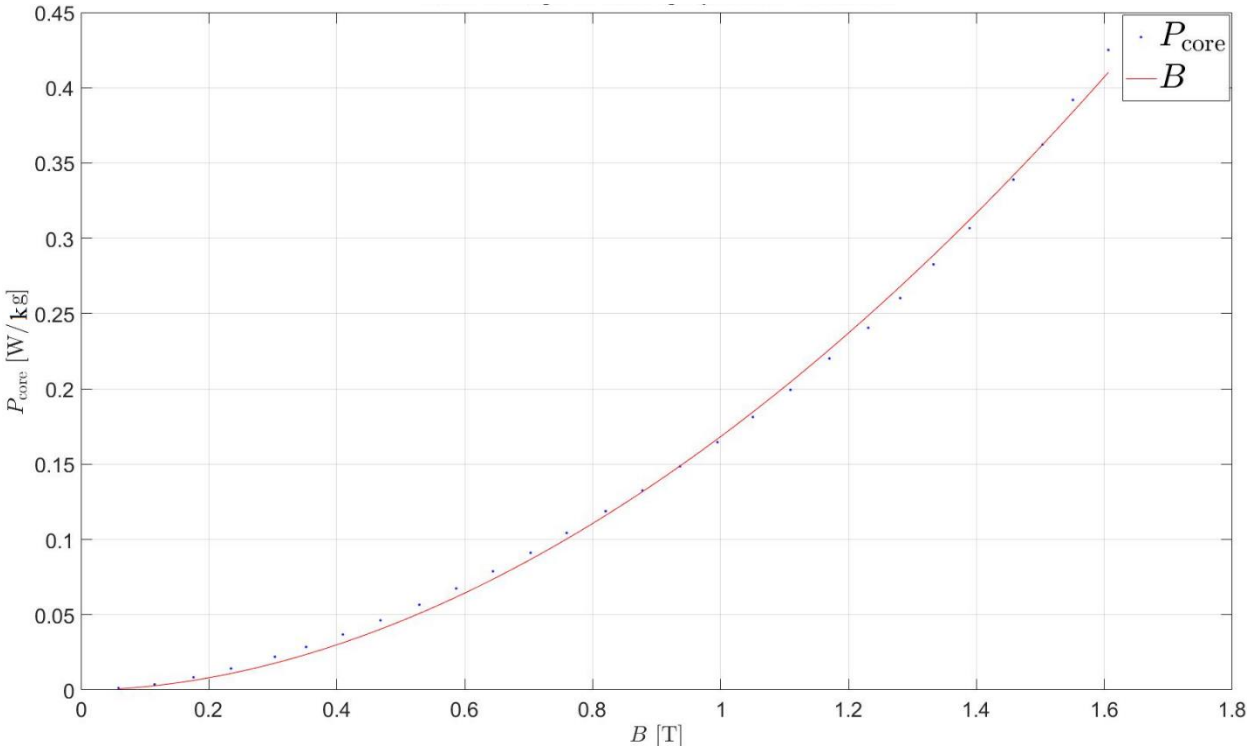

Figure 3.7: Curve fitting plot for obtaining the hysteresis coefficients

In order to obtain the eddy current loss coefficient, equation (3-22) is used for curve fitting. Measurements are done at four different frequencies (50 Hz, 100 Hz, 150 Hz, and 200 Hz) and the results are used for calculating the core losses. Then the hysteresis losses are subtracted from the core losses and the calculated values are considered as the eddy current losses. Finally, for finding the eddy current coefficients, eddy current loss versus flux density in different frequencies is plotted in order to find the eddy current coefficients.

Figure 3.8 shows a comparison between the calculated core losses in the transformer and the fitted figures for core losses in different frequencies. With increasing the frequency, the value of the core loss is increased and the behavior of the fitted and measured core loss graphs are almost the same.

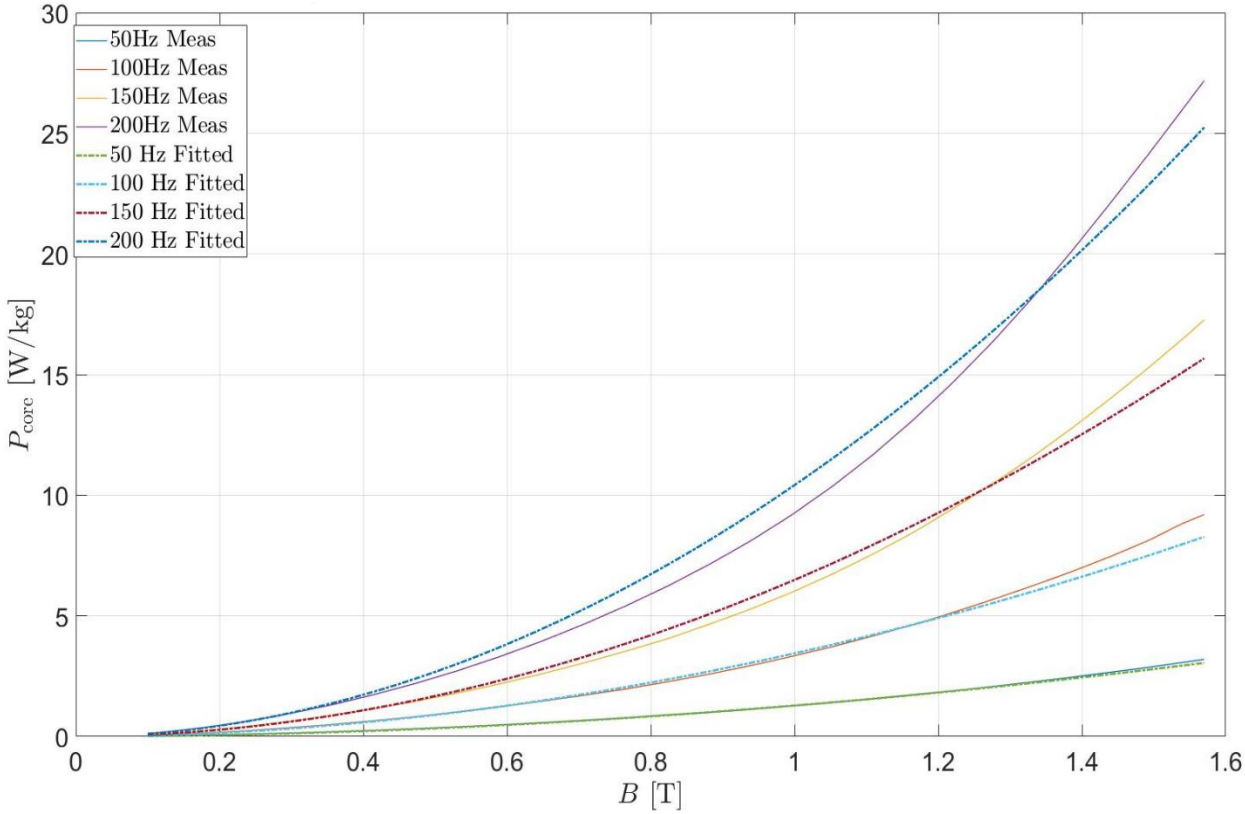

Figure 3.8: Comparison between the fitted and calculated core loss in the transformer at no-load condition

4 Electromagnetic Model

4.1 Introduction

COMSOL Multiphysics 5.3a is used to obtain a 3D transformer electromagnetic and thermal model in this thesis. There is a strong dynamic interaction between electrical and magnetic subsystems in a transformer. For designing the interaction between electrical and magnetic fields, finite element method (FEM) is used which is a powerful tool for creating the interaction between external electrical source and load in the secondary winding as well as magnetic subsystem [12]. Figure 4.1 shows the diagram of the different stages of the thesis. The electromagnetic model is used in order to obtain the core loss of the transformer. The core loss obtained from the electromagnetic model is injected into the thermal model in order to find the temperature rise in the transformer. This temperature rise is compared with the temperature rise measurement in the lab.

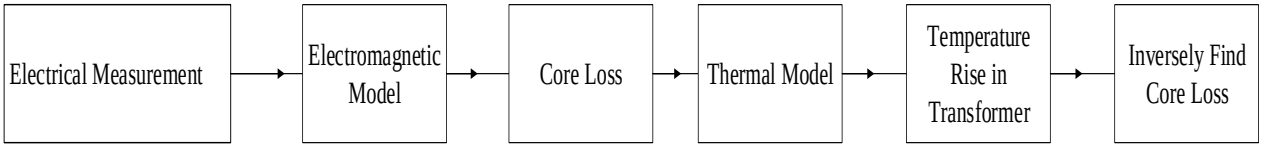

Figure 4.1: Diagram of the different stages of the thesis

4.1.1 Finite Element Method (FEM)

FEM is a numerical method for solving problems in different areas of engineering like electromagnetic or thermodynamics problems. In FEM, we divide a complex problem to smaller and simpler problem areas which are called element. Then instead of solving the problem in a complex area, we solve it in a small area. The geometry after this division is called mesh. The size of the mesh depends on the level of accuracy we need as well as computation time. The fundamental physical laws in FEM are Gauss law, Faraday law, and Ampere law which will be discussed later in this chapter [13].

4.1.2 Homogenization Approach

In order to reduce the eddy current loss in transformers, laminated core sheets are used. These laminated core sheets are the biggest problem in the modeling of a transformer with finite analysis method. It is impossible to model all of these sheets. The reason is clear. It will increase the computation effort hugely due to the large number of modeled elements. Homogenized method is an alternative approach in the finite element method for modeling the transformer. In this method, one solid structure used instead of lamination sheets. The most critical criterion is that the electromagnetic behavior of a solid structure must be the same as the laminated structure. When the conductivity is adjusted in a way that ohmic resistance of the solid domain

is equal to the eddy current path of the laminated core, the electromagnetic behavior of the homogenized structure is like laminated structure. In this thesis, we used this structure for modeling the transformer electromagnetically and compared the core loss result with the experiment. [14].

4.2 Electromagnetic Model

Figure 4.2 depicts the transformer that is used both in the lab for the measurements and simulation with COMSOL Multiphysics**.** The core of the transformer is made by laminated sheets and the transformer consists of two windings. The magnetic field intensity and flux density derived from the Ampere's law and the law of induction voltage respectively [12]. The number of primary and secondary windings are 207 and 115 turns respectively, as the transformer in the lab. The number of sheets is set 47 in COMSOL, like the transformer.

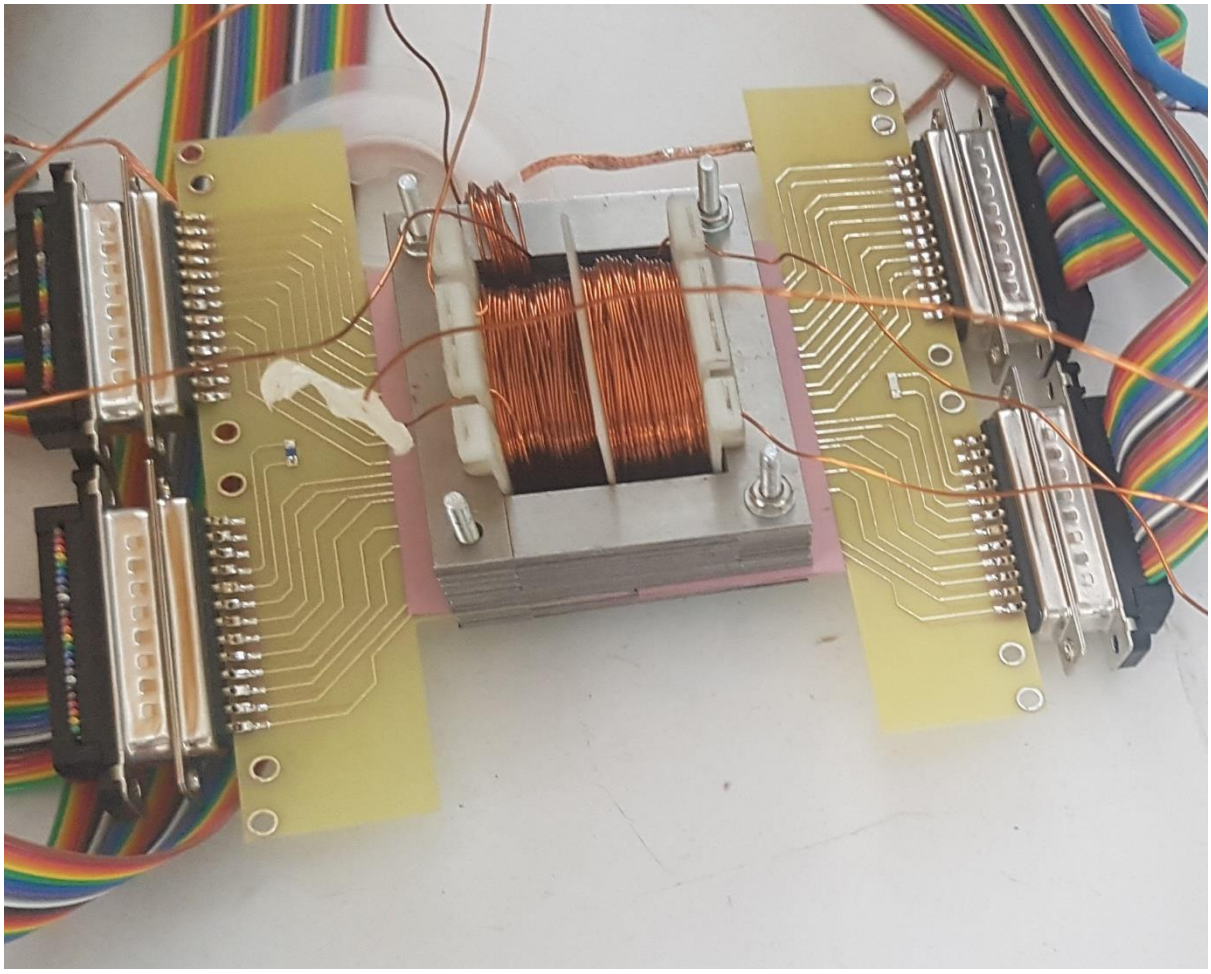

Figure 4.2: Designed transformer in the lab

At first, the material properties are defined for the different parts of the transformer. We can use COMSOL library in order to define accurate material properties for winding, transformer core, and air gap. Copper is defined in order to model the primary and secondary winding. Also, air and soft iron are used for modeling the air gap and the transformer core sheets.

mf mode is used in COMSOL Multiphysics because of the non-linear behavior of the ferromagnetic material of the core. This non-linearity of the ferromagnetic material is the reason that the problem cannot be solved in the frequency domain. On the other hand, *mf* mode in COMSOL Multiphysics allows us to do a time-dependent analysis.

As discussed earlier, the core is modeled as a homogenized structure. The transformer fed by a voltage source in the primary and the current found iteratively in each time step. This leads to higher computation time. For coupling the transformer model and external circuit in the primary, *External I Vs. U* is used in the COMSOL Multiphysics. The same had been done for the secondary winding too. Also, element *Resistor* is used for modeling the resistance of the windings in the primary and secondary. Figure 4.3 shows the mesh of transformer geometry in the electromagnetic model. We modeled one-fourth of the transformer in order to decrease the computation time in COMSOL. Appropriate boundary conditions should be defined as well which is discussed in this chapter. The non-linear magnetic behavior of the transformer core has to be considered. In constitutive relation, we used $\mathbf{H}=f(|\boldsymbol{B}|)\frac{\mathbf{B}}{|\boldsymbol{B}|}$ form [14].

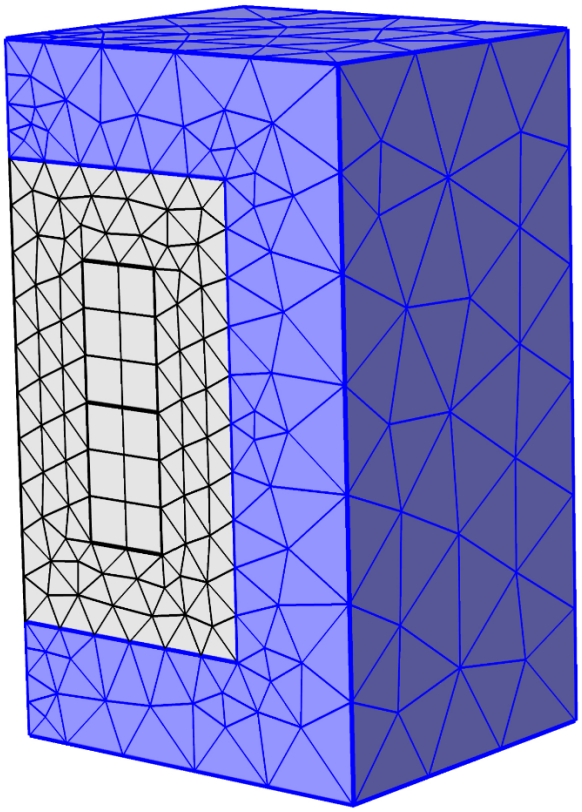

Figure 4.3: Mesh of Geometry

4.3 Maxwell's Equation

Maxwell's laws or Maxwell's equations consist of four equations that describe the interaction between the electric and magnetic fields. Gauss' law, Gauss' magnetism law, Faraday's law, and Ampere's law are the four important equations called Maxwell's equation. COMSOL Multiphysics uses Maxwell's equations in the electromagnetic model of the transformer.

4.3.1 Gauss' Law

The first Maxwell's equation is Gauss' law for the electric field. Equation (4-1) is the Gauss' law for electricity.

$$\vec{\nabla}.\vec{\mathbf{D}} = \rho \tag{4-1}$$

where $\vec{D}$ is the electric flux density and ρ is the electric charge.

According to the Gauss' law, the amount of electric flux density entering or leaving a specific volume of the space is proportional to the electric charge inside of that volume. The positive sign of the electric charge density tells us that the flux leaves the volume and the negative sign of the electric charge density indicates the flux enters the volume [15].

4.3.2 Gauss' Law for Magnetic Field

The second Maxwell's equation is the Gauss' law for the magnetic field which indicates that the total magnetic flux entering a specific volume of the space is equal to the flux leaving on that volume. Mathematical equation for the Gauss' law for magnetic field is equation (4-2). Mathematically it means the divergence of the magnetic field is equal to zero in the space.

$$\vec{\nabla}.\vec{\mathbf{B}} = 0 \tag{4-2}$$

where B is the magnetic flux density. To put it simply, there are no magnetic monopoles in space [15].

4.3.3 Faraday's Law

The third Maxwell equation is Faraday's law that indicates that the varying magnetic field produces a rotating electric field around the magnetic field. Equation (4-3) is the mathematical definition of Faraday's law [15].

$$\vec{\nabla} \times \vec{\mathbf{E}} = -\frac{\partial \vec{\mathrm{B}}}{\partial \mathrm{t}} \tag{4-3}$$

4.3.4 Ampere's Law

The last Maxwell's equation is Ampere's law that indicates a current following in the magnetic field around in a closed-loop path produces a magnetic field. Equation (4-4) is the mathematical definition of the Ampere's law:

$$\vec{\nabla} \times \vec{\mathbf{H}} = \vec{\boldsymbol{J}} + \frac{\partial \vec{\mathbf{D}}}{\partial \mathrm{t}} \tag{4-4}$$

where $\vec{\mathbf{H}}$ is the magnetic field intensity, $\frac{\partial \vec{\mathbf{D}}}{\partial \mathrm{t}}$ is displacement current density and $\vec{\boldsymbol{J}}$ is current density.

The variables in four Maxwell's equations are related to each other with a set of equations that are called constitutive relations. Equations (4-5) to (4-7) are the three constitutive relations.

$$\mathbf{D} = \varepsilon\, \mathbf{E} \tag{4-5}$$

$$\mathbf{B} = \mu\, \mathbf{H} \tag{4-6}$$

$$\mathbf{J} = \sigma\, \mathbf{E} \tag{4-7}$$

Where

- ε is the permittivity of the material
- μ is the permeability of the material
- and σ is the conductivity of the material [15].

4.3.5 Boundary Condition

FEM is used for modeling the transformer in COMSOL. The finite element method is used broadly in different areas of engineering design. In the field of transformer design, FEM is being used predominantly in order to study the magnetic flux distribution, losses, and etc [16]. Because of the complexity in the transformer windings structure, 2D and 3D FEM model is widely used nowadays. Due to the symmetry, one-fourth of the transformer is modeled. The boundary conditions are defined in addition to Maxwell's equations. These different boundary conditions are the borders of the transformer and the outer environment or the interfaces within the different parts of the domain because of the different material properties (air, soft iron, and winding). Dirichlet boundary condition, Neumann boundary condition, and (anti)periodic boundary condition are defined. In the Dirichlet boundary condition, magnetic vector potential (**A**) is constant. It means the field is parallel to the boundary. In the magnetic problems, Dirichlet conditions are used to hold magnetic flux from crossing the boundary. The field is perpendicular in the Neumann boundary condition. It means in the magnetic problems, homogeneous Neumann boundary conditions make the magnetic flux pass the boundary at 90 degrees to the boundary. As we have symmetry in our model, the (anti)periodic boundary condition is defined which means at the boundaries of the interface $A_1 = \pm A_2$ satisfies [17].

4.4 Core Loss Computation

The core loss is calculated based on the electromagnetic model of the transformer in COMSOL. The model is connected to Matlab Via Livelink to MATLAB. With the help of the MATLAB, the flux density in each element of the mesh grid is found. The peak value of the flux density cannot be used for computing the core loss due to the harmonics. In each element, fast Fourier transform of magnetic field is done in order to find the weight of each harmonic component. Then the value of the core loss can be calculated based on the equation (4-8).

$$P_{\text{core}} = P_{\text{h}} + P_{\text{e}} = K_{\text{h}} B_{\text{max}}^{n} f + K_{\text{e}} B_{\text{max}}^{2} f^{2} \tag{4-8}$$

As mentioned earlier, the excess loss is ignored in this thesis. The total value of the core loss is the summation of the core loss value in each element. The calculated core loss will be used to find the temperature rise in the thermal model in the next chapter.

4.5 Simulation Result

The electromagnetic model of the transformer is built in COMSOL and the simulation results are compared with the results from the measurement. Figure 4.4 illustrates a comparison between the measured and modeled core loss in the transformer at four different frequencies (50 Hz, 100 Hz, 150 Hz, and 200 Hz) in no-load condition. Figure 4.4 shows a clear correlation between the core loss from the measurement and core loss from the electromagnetic in COMSOL. Equations (3-17) and (3-18) are used for calculating the core loss.

Figure 4.5 displays the flux distribution in the transformer. The measured primary current and secondary voltage are compared with the modeled primary current and secondary voltage in figures 4.6 and 4.7.

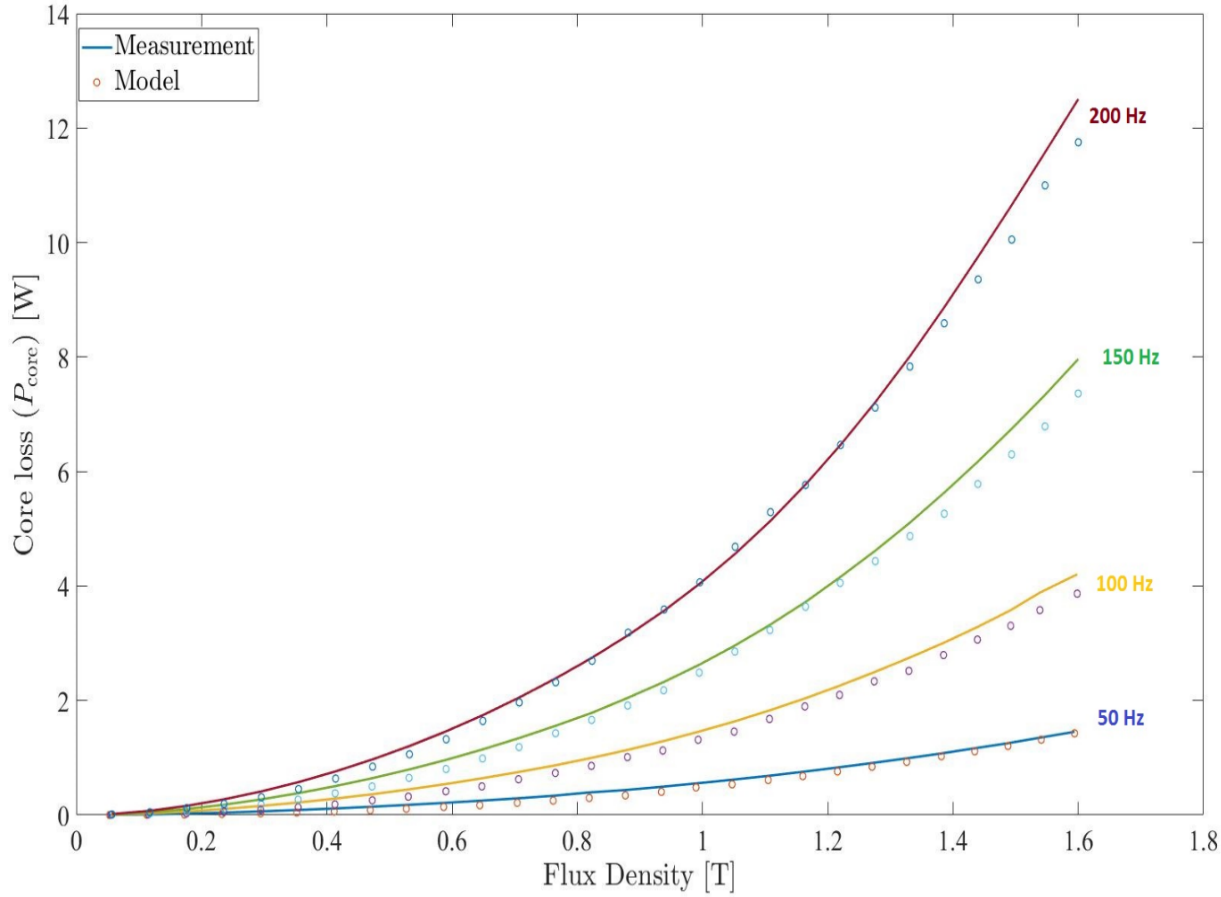

Figure 4.4: Comparison between measured and modeled core loss

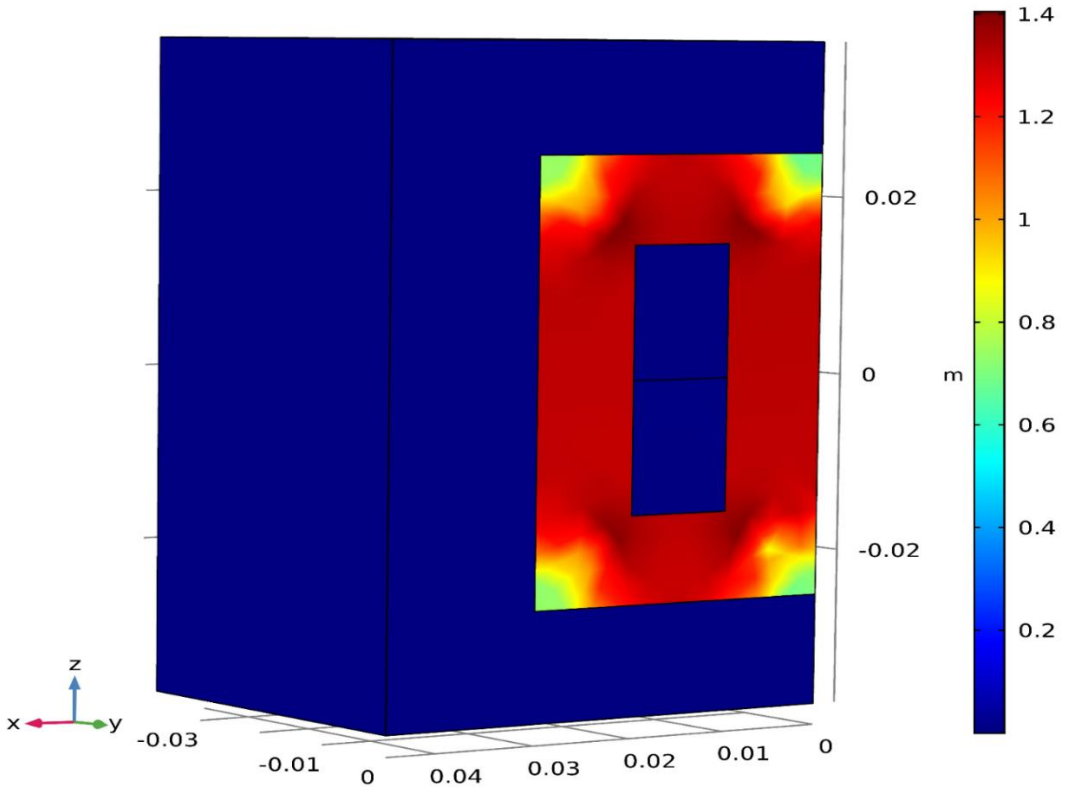

Figure 4.5: Flux distribution in the transformer

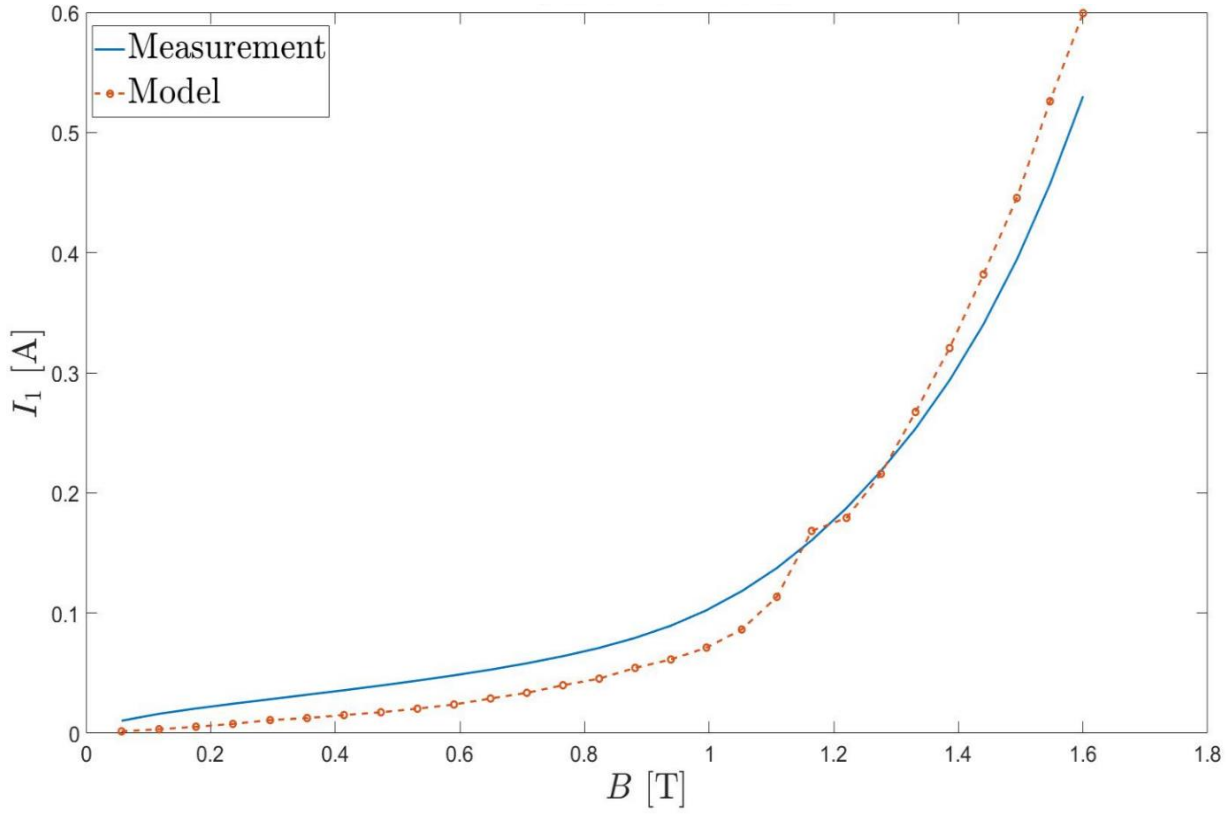

Figure 4.6: Comparison between measured and modeled primary current

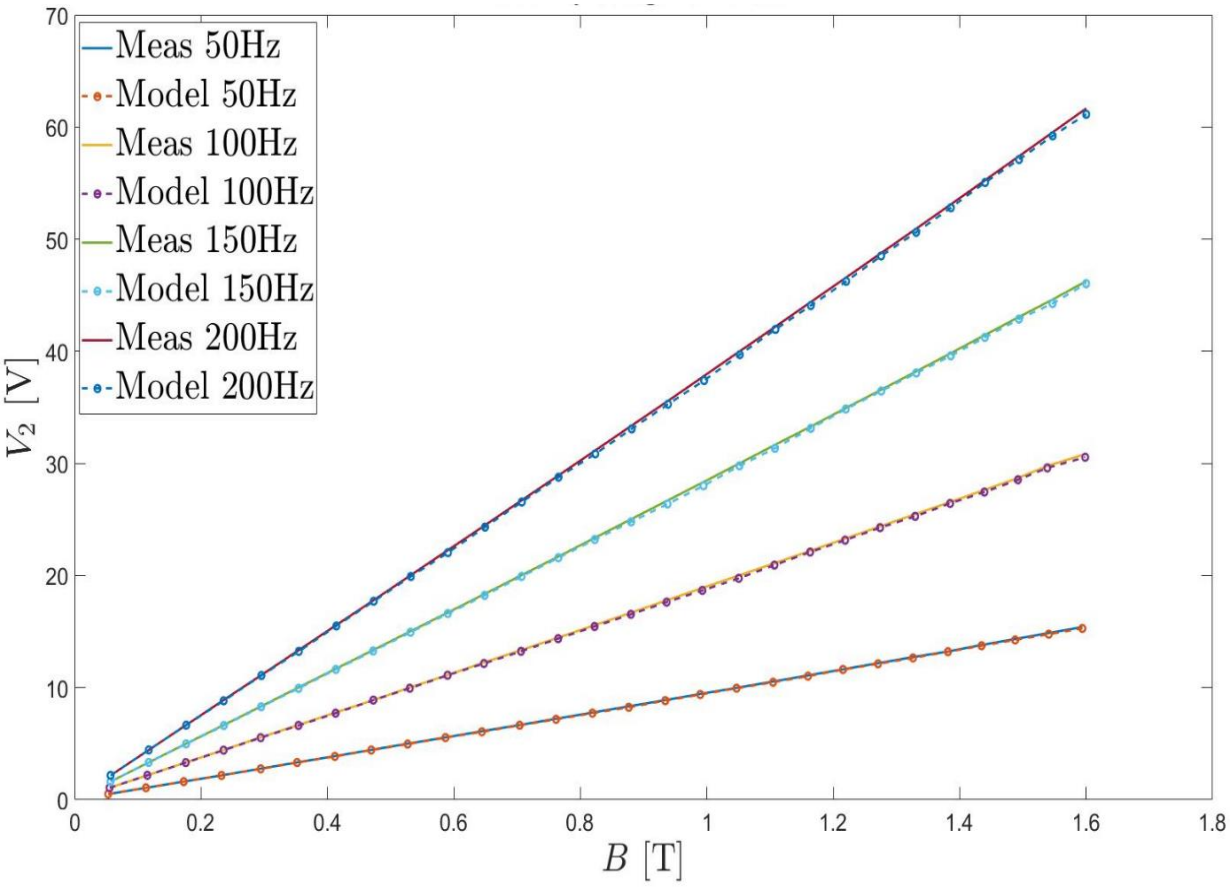

Figure 4.7: Comparison between measured and modeled secondary voltage

5 Thermal Model

5.1 Introduction

Before improvement of computers and other modeling software, analysis and design of transformers or electrical machines were limited to electromagnetic aspects. Just some constraints on the current density applied in order to avoid overheating of the transformer or electrical machines. Nowadays, one of the most important factors in designing a transformer is its efficiency. Also, the lifetime of a transformer is extremely important, for example in a power system network as they are received the majority of the investment in a network. Therefore, a deep knowledge of the thermal behavior of a transformer becomes important for having more efficient transformer [18]. Traditionally, empirical formulae from the standard as well as practical measurements in the lab were the two techniques in order to calculate the temperature rise and furthermore, loss in the transformer. In this thesis, the thermal model of the transformer is modeled based on FEM and with COMSOL. It shows the heat distribution in the transformer and how the transformer behaves when the input has been changed. Basically, thermal model is the mathematical prediction of the temperature rise in the transformer because of the losses.

Table 5.1 displays the analogy between electrical quantities and thermal quantities [19].

Table 5.1: Analogy between electrical and thermal quantities

Electrical quantities			Thermal quantities		
Potential	V	[V]	Temperature	θ	[°K]
Current	I	[A]	Heat	Q	[W]
Current density	J	$[A/m^2]$	Heat flux	q	$[W/m^2]$
Conductance	G	[S]	Thermal conductance	G_{th}	[W/K]
Conductivity	σ	[S/m]	Thermal conductivity	λ	[W/mK]
Resistance	R	[Ω]	Thermal resistance	R_{th}	[K/W]
Resistivity	ρ_r	[Ω/m]	Thermal resistivity	$\rho_{r,th}$	[mK/W]
Capacitance	C	[F]	Thermal Capacitance	C_{th}	$[J/°K]$

In the first section of this chapter, a brief result of the temperature rise measurements are introduced. Then, a general theory about heat transfer is presented. The method and equations that are used in the thermal model are discussed and at the end, a comparison between the temperature rise from the model and the measurement is presented.

5.2 Lab Measurement

Temperature rise measurements in different frequencies are done in the lab. PT 100 is used as a temperature sensor in this thesis. The temperature sensor sheet contains 10 sensors in different locations that measure the temperature rise in different areas of the transformer. The sensors located in the middle of the transformer. Figure 5.1 shows the location of the temperature sensors inside the transformer core. The temperature sensor sheet has 10 sensors that are located like figure 5.1 inside the transformer core. The 10^{th} sensor is located outside of the transformer. Figure 5.2 shows the temperature rise in the central limb of the transformer at no-load at different frequencies. By increasing the frequency of the power source, the induced emf voltage in the core will be increased which leads to higher circulating currents. Therefore, the value of the eddy current loss increases and it leads to a higher rise in the temperature of the transformer. Figure 5.2 shows only the temperature rise in the central limb of the transformer, but the temperature rise on the other parts of the transformer have almost the same pattern.

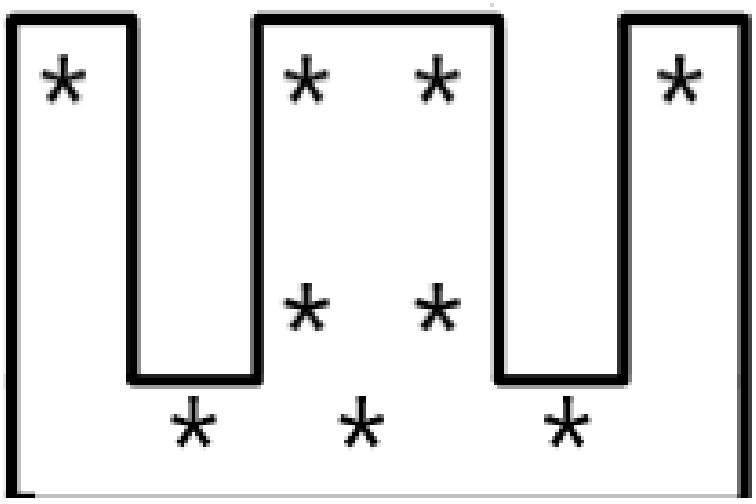

Figure 5.1: Location of the PT-100 temperature sensor inside the transformer core

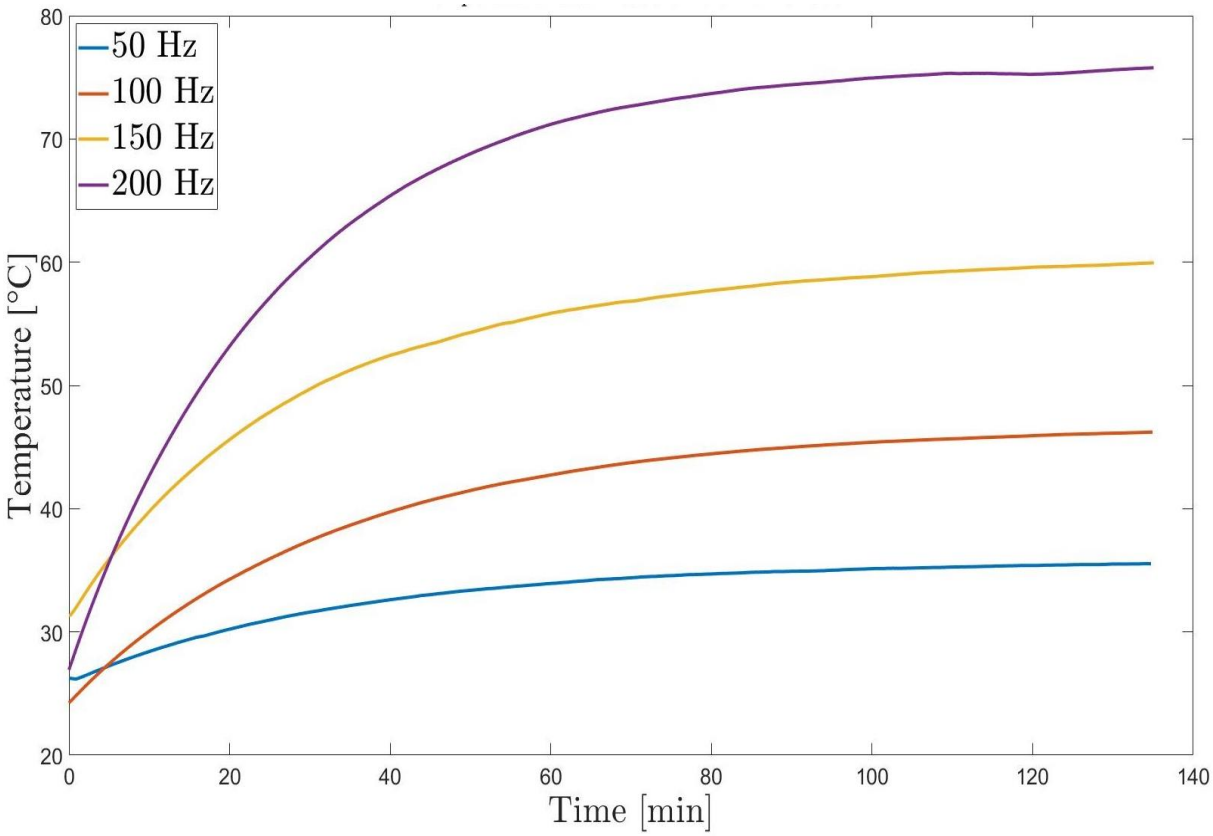

Figure 5.2: Central limb temperature rise at no-load

5.3 Heat Transfer

The second law of thermodynamics tells the temperature difference evens out with the transferring of the heat from the point with the higher temperature to the point with lower temperature. The temperature rise in a transformer leads to an increase in the resistance of the winding and as a result, it increases the losses [21]. Equation (5-1) is used for evaluation of the temperature in finite element thermal model of the transformer.

$$\frac{\partial}{\partial x}\left(k_{\mathrm{x}}\frac{\partial T}{\partial x}\right)+\frac{\partial}{\partial y}\left(k_{\mathrm{y}}\frac{\partial T}{\partial y}\right)+\frac{\partial}{\partial z}\left(k_{\mathrm{z}}\frac{\partial T}{\partial z}\right)+q=\rho C_{\mathrm{p}}\frac{\partial T}{\partial x} \tag{5-1}$$

where q is the heat generated in the transformer due to the losses and k_{x}, k_{y}, and k_{z} are the thermal conductivities in x, y, and z direction. The value of q is calculated with the help of the electromagnetic model.

Heat transfer consists of three main transfer mechanisms that are presented in the following subsections [18].

5.3.1 Conduction

Heat transfer can occur in two different ways by conduction: by free electrons and molecular interaction. The first one usually occurs in the pure metals where there are some free electrons in alloys. The latter is more typical in gases, liquids, and solids. In that case, molecules at the higher energy levels that have higher temperature release energy for the molecules at the lower energy levels by lattice vibration [21]. The temperature difference between two different systems that have a thermal contact leads to heat transfer usually from higher temperature area to the lower temperature area. The conduction heat transfer rate $q_{\mathrm{h}}$is proportionally related to the thermal conductivity of the material, [W/mK], the temperature gradient in the heat flow direction (∇T) and the heat transfer cross-sectional area (A).

$$q_{\mathrm{h}} = -k_{\mathrm{h}} A \nabla \mathrm{T} \tag{5-2}$$

Where k_{h} is the thermal conductivity of the material.

Equation (5-2) represents the Fourier law of conduction. The negative sign in the equation tells the heat transfer is from the higher temperature area towards the lower temperature area. The differential heat equation for any point of the material will be available when we apply the rule of energy balance. Therefore:

$$\rho C_{\mathrm{p}} \frac{\partial T}{\partial t} = Q_{\mathrm{h}} + \nabla.(k_{\mathrm{h}} \nabla T) \tag{5-3}$$

where

- Q_{h} is the power generated per unit volume [$\mathrm{W/m^3}$].
- ρ is the material density [$\mathrm{kg/m^3}$].
- C_{p} is the specific heat capacity [J/kg K].

The left hand side of the equation (5-3) is zero in steady-state [18].

5.3.2 Convection

Fluid motion is the reason for the heat convection. In other words, the difference between the temperature of the body surface and fluid over the surface cause the convection of heat. Heat convection can be divided into two types. Natural convection or forced convection. The first one is because of the density difference in the fluid. The temperature difference on the body surface or by heat conduction leads to the density difference in the fluid. To put differently, the natural convection is the fluid motion that is not created by the external sources like a fan. It is only because of the density differences. The latter one is the convection created by the external sources like fan or pump. Convection is described by Newton's law of cooling [20].

$$q_{\mathrm{h}} = h_{\mathrm{c}} A_{\mathrm{cv}} (T_{\mathrm{s}} - T_{\mathrm{amb}}) \tag{5-4}$$

where

- q_{h} is heat transfer rate [W].
- h_{c} is the heat transfer convection coefficient [$\mathrm{W/m^2K}$].
- A_{cv} is the surface area of the surface exposed to the fluid flow [$\mathrm{m^2}$].
- T_{s} is the surface temperature [K].

- T_{amb} is the ambient temperature [K].

5.3.3 Radiation

Heat transfer by radiation is different from the heat transfer from convection and conduction. It occurs in the form of electromagnetic waves and represents the conversion of the thermal energy into electromagnetic energy. When an object getting warm, its molecules start to move. With an increase in the temperature of that object, the vibration of the molecules going up and leads to accelerating the electric charges of the object. In contrast to the other two mechanisms of the heat transfer, radiation does not need a medium for heat exchange. When the heat radiated to an object, it can be absorbed by the object, or reflect backward or transmit through the object [21].

The radiation heat transfer is described by the Stefan-Boltzmann law of radiation:

$$q_{\mathrm{h}} = \epsilon \sigma_{\mathrm{B}} A (T_{\mathrm{s}}^4 - T_{\mathrm{rad}}^4) \tag{5-5}$$

where

- q_{h} is the heat transfer rate from the object surface.
- ϵ is the emissivity of the radiating surface.
- σ_{B} is the Stefan-Boltzmann constant, $\sigma_{\mathrm{B}} = 5.67 \times 10^{-8}\ \mathrm{W/m^2K^4}$.

The value of the σ_{B} is very low. So the heat transfer by radiation can be neglected when the difference of the T_{s} and T_{rad} are small [20].

5.4 Thermal Model in Comsol Multiphysics

Comsol Multiphysics is used for modeling the transformer. Figure 5.3 shows the thermal model of one-quarter of the transformer. One of the most important factors that we need to know before model the transformer is thermal properties of magnetic material. The total thermal behavior of the transformer depends on the thermal properties of each part of the transformer, like air, soft iron, and copper. The thermal properties of the different elements of the transformer are summarized in table 5.2.

Table 5.2: Properties of the materials

Transformer part	Material	Mass density $[\mathbf{kg/m^3}]$	Heat capacity $[\mathbf{J/kg\,K}]$	Thermal conductivity $[\mathbf{W/mK}]$
Air gap	Air	1.225	1005	0.0254
Core	Steel	7850	580	28
Windings	Copper	8940	385	400

Modeling of Anisotropic thermal properties of materials in the thermal finite element model of a transformer is very important. The thermal conductivity of the core and windings are modeled using the Hashin and Shtrikman approximation [20]. The thermal conductivity of the copper winding is modeled in two directions: Thermal conductivity in lapping direction and thermal conductivity in perpendicular to lapping direction.

$$K_{\mathrm{hwp}} = \begin{cases} f_{\mathrm{p}} K_{\mathrm{h_c}} + \left(1 - f_{\mathrm{p}}\right) K_{\mathrm{h_a}}\,, & \text{In lapping direction} \\ K_{\mathrm{h_a}} \dfrac{(1+f_{\mathrm{p}})K_{\mathrm{h_c}} + \left(1-(1-f_{\mathrm{p}})\right)K_{\mathrm{h_a}}}{(1-f_{\mathrm{p}})K_{\mathrm{h_c}} + \left(1+(1-f_{\mathrm{p}})\right)K_{\mathrm{h_a}}}\,, & \text{In perpendicular direction} \end{cases} \tag{5-6}$$

where

- f_{p} is filling factor for primary
- $K_{\mathrm{h_c}}$ is thermal conductivity of copper
- $K_{\mathrm{h_a}}$ is thermal conductivity of air

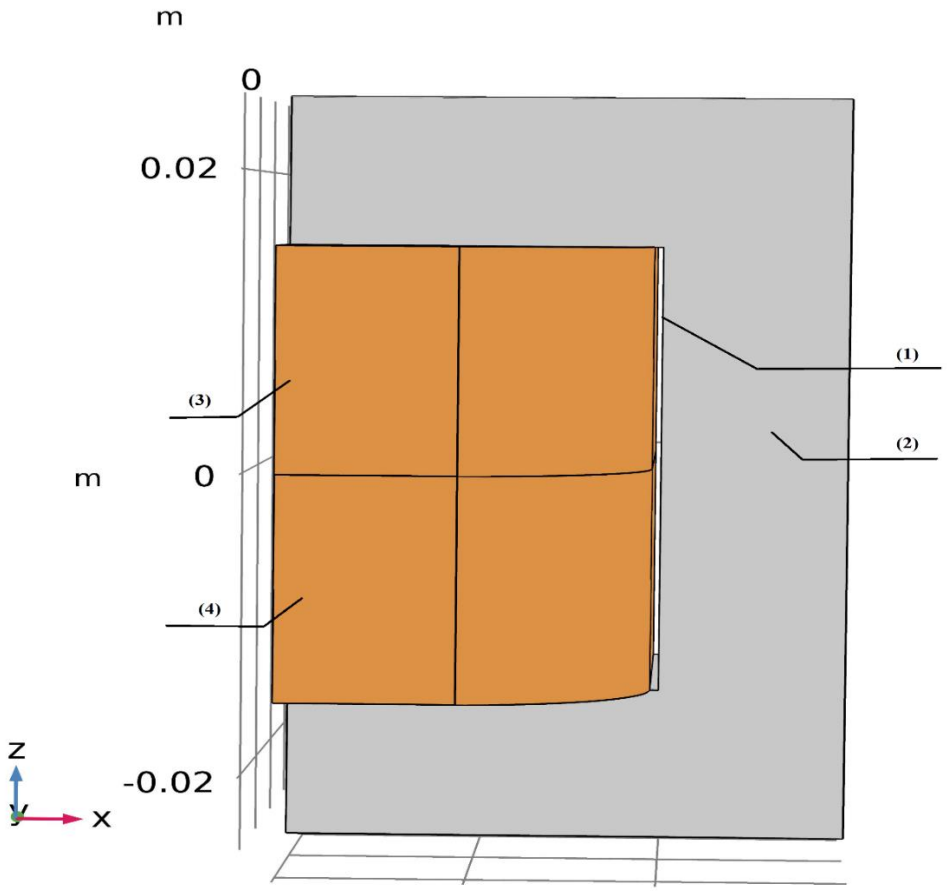

Figure 5.3: Thermal model of the one-quarter of the transformer. (1) Air gap, (2) Homogenous iron core, (3) Primary winding, (4) Secondary winding.

Equation 5-6 is the primary winding thermal conductivity (K_{hwp}). In order to obtain the thermal conductivity equation for the secondary winding, the filling factor value of the primary winding in the equation 5-6 is substituted with the filling factor of the secondary winding.

$$K_{\mathrm{hws}} = \begin{cases} f_{\mathrm{s}}K_{\mathrm{h_c}} + (1-f_{\mathrm{s}})K_{\mathrm{h_a}}\,, & \text{In lapping direction} \\ K_{\mathrm{h_a}}\frac{(1+f_{\mathrm{s}})K_{\mathrm{h_c}}+(1-(1-f_{\mathrm{s}}))K_{\mathrm{h_a}}}{(1-f_{\mathrm{s}})K_{\mathrm{h_c}}+(1+(1-f_{\mathrm{s}}))K_{\mathrm{h_a}}}\,, & \text{In perpendicular direction} \end{cases} \tag{5-7}$$

where

- K_{hws} is the secondary winding thermal conductivity.
- f_{s} is the secondary winding filling factor.

The heat capacity of the primary and secondary windings is presented as a function of the filling factor.

$$C_{\mathrm{pwp}} = f_{\mathrm{p}} C_{\mathrm{pc}} + (1 - f_{\mathrm{p}}) C_{\mathrm{pa}} \tag{5-8}$$

$$C_{\mathrm{pws}} = f_{\mathrm{s}} C_{\mathrm{pc}} + (1 - f_{\mathrm{s}}) C_{\mathrm{pa}} \tag{5-9}$$

where

- C_{pwp} is the heat capacity of the primary winding.
- C_{pws} is the heat capacity of the secondary winding.
- C_{pc} is the heat capacity of the copper.
- C_{pa} is the heat capacity of the air.

Finally, the mass density of the windings needs to be presented:

$$\rho_{\mathrm{wp}} = f_{\mathrm{p}} \rho_{\mathrm{c}} + (1 - f_{\mathrm{p}}) \rho_{\mathrm{a}} \tag{5-10}$$

$$\rho_{\mathrm{ws}} = f_{\mathrm{s}} \rho_{\mathrm{c}} + (1 - f_{\mathrm{s}}) \rho_{\mathrm{a}} \tag{5-11}$$

where

- ρ_{wp} is the mass density of the primary winding.
- ρ_{ws} is the mass density of the secondary winding.
- ρ_{c} is the mass density of the copper.
- ρ_{a} is the mass density of the air.

Equations (5-6) to (5-11) are for the windings of the transformer. The same is done for the modeling of the transformer core. The filling factor of the winding is replaced by the filling factor of the core which is almost 0.95.

Figure 5.4 illustrates the windings of the transformer. In order to define the thermal conductivity of the windings, we divided each winding into five parts as shown in figure 5.4.

In part (1), the wires are wound in the x-direction. There is insulation between each wire. Therefore, in the model, the value of the thermal conductivity in the y-direction and z-direction is defined very low. The same rule applied for the part (5) of the primary winding of the transformer. Part (3) is also considered as a straight area and the value of the thermal conductivity in the y-direction is hugely higher than in x-direction and z-direction. Thermal conductivity values for the part (2) and (4) are not in one direction. Equation 5-12 is used for finding the value of conduction:

$$q_{\mathrm{i}} = -k_{\mathrm{ij}} \nabla T_{\mathrm{j}} \tag{5-12}$$

Where k_{ij} is the second-order thermal conductivity tensor. For the material with isotropic thermal conductivity, $i = j$. In the case of isotropic thermal conductivity, the heat flux follows in the direction of the temperature gradient. But in the case of anisotropic, the temperature gradient in y-direction or z-direction affect the heat flux in the x-direction. Equation (5-13) shows the new equation for the thermal conductivity:

$$k_{\mathrm{ij}}^{\mathrm{n}} = \frac{J k_{\mathrm{ij}} J^{T}}{\det(J)} \tag{5-13}$$

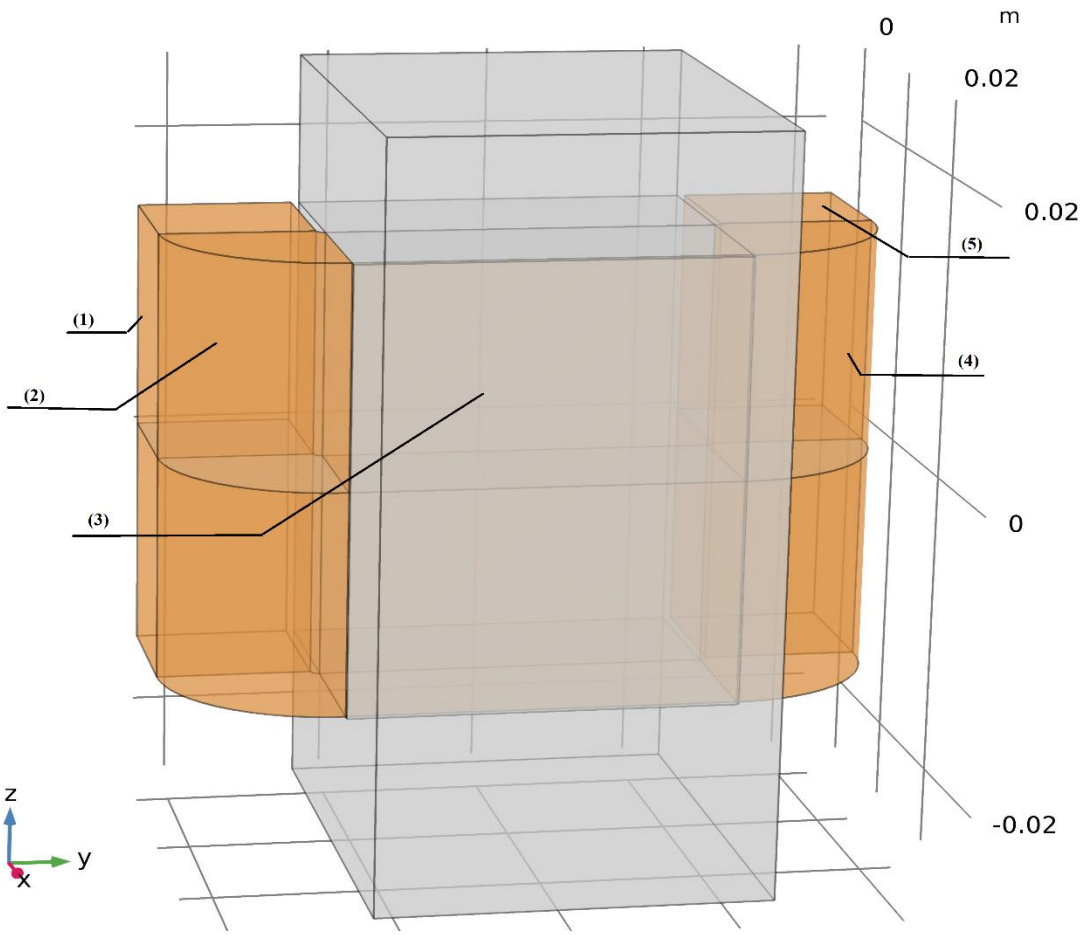

Figure 5.4: Windings of the transformer in the thermal model

Where J is the Jacobian matrix of the coordinate transformation from the old coordinate system to the new coordinate system.

$$J = \begin{bmatrix} \cos(\theta) & \sin(\theta) & 0 \\ -\sin(\theta) & \cos(\theta) & 0 \\ 0 & 0 & 1 \end{bmatrix} \tag{5-14}$$

When the rotation is around the z-axis. J^T is the transpose of the Jacobian matrix.

Finally, the relevant physics is added to the model for computing the temperature distribution of the transformer model. From COMSOL physics library, heat transfer in the solid interface is added to the model. It can model the heat temperature distribution based on conduction, convection, and radiation. Also, the respective symmetric boundary condition is applied to the model, as one-fourth of the transformer is modeled. The heat source in the transformer is divided into two groups. First one is the core loss which is taking place in the core of the transformer and the second one is copper loss which occurs in the primary and secondary windings of the transformer. Core loss is obtained from the electromagnetic model in the previous chapter and the obtained value is injected to the thermal model as a heat source. As the resistance will increase with the rise of the temperature, the copper loss should be defined as a function of temperature. Equation (5-15) shows the copper loss as a function of temperature rise.

$$P_{\mathrm{cu}} = P_{\mathrm{w}}\big(1 + \alpha(T - T_{\mathrm{amb}})\big) \tag{5-15}$$

where α is the temperature coefficient of resistance for copper and is equal to 0.004041. T is the temperature of the winding and T_{amb} is the temperature of the ambient. Then the mesh of geometry is created in order to solve the differential equation regarding the heat transfer in FEA.

5.5 Simulation result

The core loss result from the electromagnetic model is injected into the thermal model of the transformer. Figure 5.5 shows the heat distribution in the transformer at full load and 100 Hz as the supply frequency. Temperature in the secondary winding is higher due to the fact that the secondary current is higher than the primary current, and therefore, the loss in the secondary winding is higher than the primary. Due to the fact that in the full load condition, the transformer is heating up because of both core loss and winding loss, the temperature rise in the winding is higher than the core [22].

Figures 5.6 compared the temperature rise of the transformer model in COMSOL with the measured temperature rise in the lab. The measurement has been done for about 80 to 100 minutes in full load condition and at 100 Hz as supply frequency. There is good agreement between the measured temperature rise graphs of the transformer and the modeled one for both primary winding and secondary winding. However, due to the fact that the value of the air convection in the model is not exactly accurate, there is a very small difference between graphs.

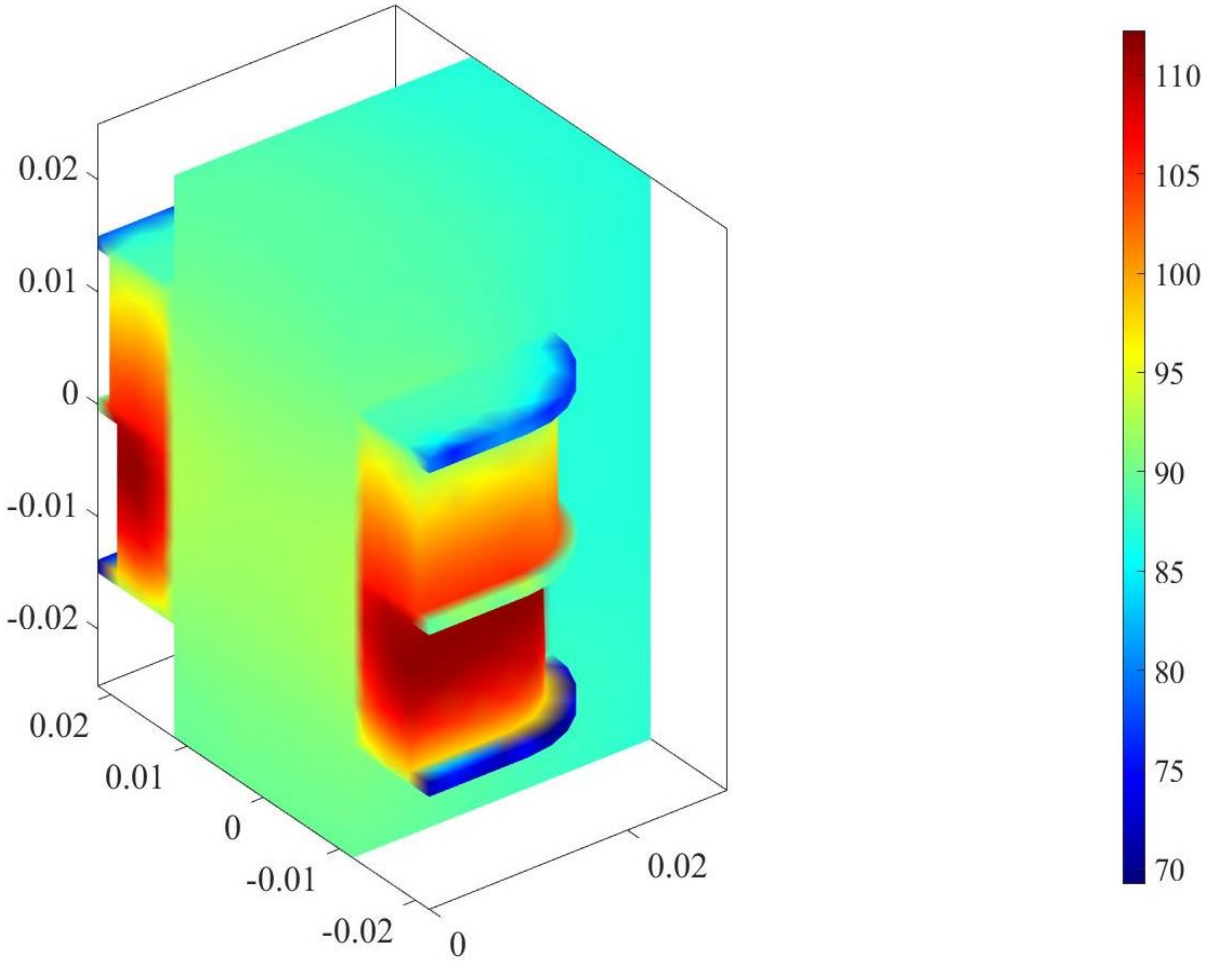

Figure 5.5: Heat distribution in the transformer model

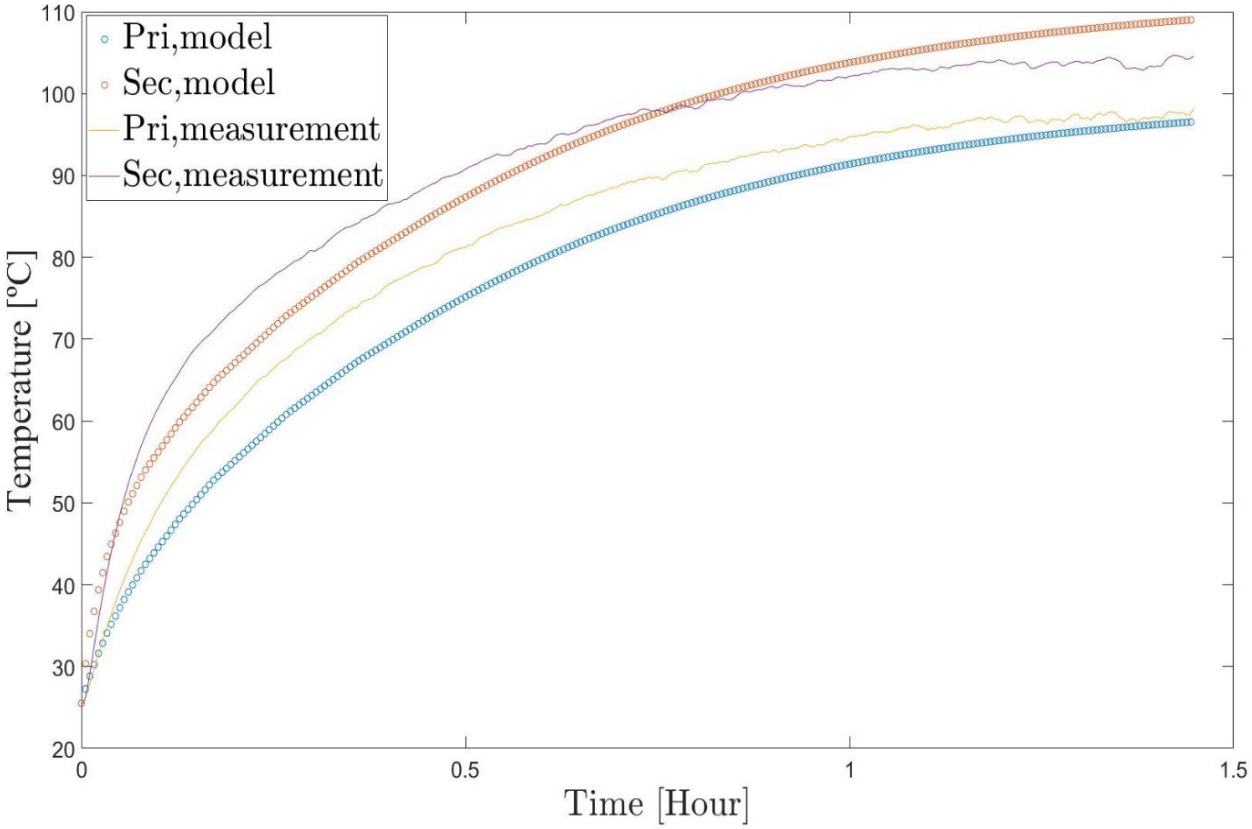

Figure 5.6: Temperature rise comparison between the measurement and COMSOL model at 100 Hz in full load condition

6 Conclusion and Future Work

6.1 Conclusion

The main objective of the thesis is to develop the electromagnetic model and the thermal model of the transformer and compare the results with the data from the measurements. The traditional way of obtaining losses in the transformer could be affected by a lot of factors. High harmonics can have a negative effect on the power analyzer and as a result, inaccurate losses measurement. Moreover, if a transformer supplied from a PWM inverter fed supply, the power analyzer will be inaccurate in power losses computation. The first task was to design a transformer within the required specification in the lab. No load and loaded measurements have been done in the lab in four different frequencies and the results are used for calculating the core loss in the transformer. Afterward, the hysteresis and eddy current loss were found based on the measurement data with the help of Steinmetz equation. Excess loss is neglected in this thesis and hysteresis and eddy current losses are supposed to form the core loss of the transformer. The electromagnetic model is developed in COMSOL Multiphysics in order to obtain the core loss in the electromagnetic model and compare it with the core loss obtained by the measurements. The electromagnetic model is based on the solution of Maxwell's equation and imposing this solution to eddy currents and hysteresis coefficients to obtain the losses.

At the third phase of the thesis, the thermal model is developed in COMSOL Multiphysics. The core loss results from the electromagnetic model are injected to the thermal model to obtain the value of the temperature rise in the primary winding, secondary winding, and transformer core. The values of convection are not easy to define, as they are not equal for the whole part of the winding. Also, the air gap was one of the most important parts of the transformer model. Due to the high thermal resistance of the air, it can have an effect on the thermal behavior of the transformer.

The final test was comparing the temperature rise values obtained from the thermal model with the temperature rise of the transformer in the lab. The transformer was run for about 90 minutes and the temperature of the transformer was measured by the PT 100 temperature sensors which were located in the middle of the transformer. The obtained values for temperature rise based on the measurements have good agreement with the values from the thermal model. However, there is some small difference in steady-state temperature which is due to some factors like convection coefficient values.

6.2 Future Work

As discussed earlier, in order to obtain the loss in the transformer, measurement devices were used. High harmonics can affect the quality of the measurement. But, the temperature rises of the transformer are independent of such issues. Therefore, measuring the temperature rise and obtaining the transformer loss inversely from the temperature rise is a more accurate approach for obtaining the loss in the transformer.

References

[1] Chapman, S.J., 2011. *Electric Machinery Fundamentals.* McGraw-Hill Education.

[2] Chen, Y., Pillay., 2002. An improved formula for lamination core loss calculation in machines operating with high frequency and high flux density excitation. *in Conf Rec. 37th IEEE IAS Annu. Meeting,* 2002,vol. 2, pp. 759–766.

[3] D.G.Nair and A.Arkkio, "Inverse thermal modeling to determine power losses in induction motor," IEEE Trans. Magn., vol. 53, no. 6, June. 2017, Art. no. 8103204.

[4] H.Bahmani, "Development of novel techniques for the assessment of inter-laminar resistance in transformer and reactor cores," *PhD dissertation, Cardiff University,* 2014.

[5] Kothari, D.P., Nagrath, I.J., 2010."*Electric Machines"* McGraw-Hill India.

[6] R.G.Carter,*" Electromagnetism for electronic engineers".* Springer, 1992.

[7] S.B. Guru and H.R. Hiziroglu, "*Electric Machinery and Transformers".*Oxford University Press, 2000.

[8] P.C.Sen, "*Principle of electric machines and power electronics",* Wiley India, 2000.

[9] D.P.Lammeraner and M.Stafl. *"Eddy currents",* Iliffe, 1967.

[10] F.Marketos, D.Marnay, T.Ngnegueu, *"Experimental and numerical investigation of flux density distribution in the individual packets of the 100 kVA transformer core,"* Magnetics IEEETransactions on, 2012, 48(4):1677-1680.

[11] P.Parthasaradhy and S.V.Ranganayakulu, "*Hysteresis and eddy current losses of magnetic material by Epstein method-novel approach*," IJES, 2014, 2319-1813, Page 85-93.

[12] H. Neubert, T. Bödrich, R. Disselnkötter," Transient Electromagnetic-Thermal FE-Model of a SPICE-Coupled Transformer Including Eddy Currents with COMSOL Multiphysics 4.2," *2011 COMSOL conference in Stuttgart.* 5th European COMSOL Conference, Stuttgart (D), 26.-28.10.2011.

[13] G. Meunier, "*The Finite Element Method for Electromagnetic Modeling"* Wiley-ISTE; 1 edition, 2008.

[14] H. Neubert, J. Ziske, T. Heimpold, R. Dissenlötter, "Homogenization Approaches for Laminated Magnetic Cores using the Example of Transient 3D Transformer Modeling," *COMSOL conference in Rotterdam.* 2013.

[15] D. Fleisch, "*A Student's Guide to Maxwell's Equations (Student's Guides)",* Cambridge University Press (January 28, 2008).

[16] L. Naranpanawe, C. Ekanayake, "Applications of FEM in condition monitoring of transformer clamping system", *Australasian Universities Power Engineering Conf., Melbourne, Australia,* November 2017, pp. 1–6.

[17] D.Padhiyar, "Analysis of single-phase transformer using FEMM,"*IJIRT,* Volume 4, Issue 12, May 2018.

[18] D. Kowal, "Methodology to evaluate the influence of electrical steel properties on the design of wind turbine generators", *PhD dissertation, Ghent University,* 2013.

[19] N. Nisar, "Structural Optimization and Thermal Modeling of Flux Switching Machine", *Master thesis, Aalto University,* 2015.

[20] A. Hemeida, "Electromagnetic and Thermal Design of Axial Flux Permanent Magnet Synchronous Machines", *PhD dissertation, Ghent University,* 2017.

[21] J. Pyrhonen, T. Jokinen, and V. Hrabovcova, ” *Design of rotating electrical machines”,* John Wiley Sons, 2013.

[22] M. Mogorovic, D. Dujic, “ Thermal modeling and experimental verification of an air-cooled medium frequency transformer”, in *19th European Conference on Power Electronics and Applications (EPE),* 2017.